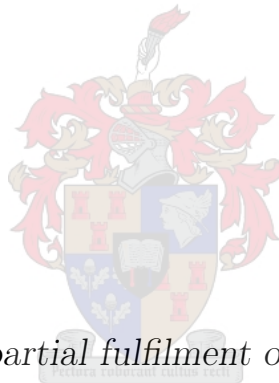# The role of a positive feedforward loop in regulating yeast glycolytic intermediate dynamics

by

Soné Kotze

Thesis presented in partial fulfilment of the requirements for the degree of Master of Science (Biochemistry) in the Faculty of Science at Stellenbosch University

Supervisor:	Prof. J.L. Snoep
Co-supervisor:	Dr. D.D. van Niekerk

December 2021

Declaration

By submitting this thesis electronically, I declare that the entirety of the work contained therein is my own, original work, that I am the sole author thereof (save to the extent explicitly otherwise stated), that reproduction and publication thereof by Stellenbosch University will not infringe any third party rights and that I have not previously in its entirety or in part submitted it for obtaining any qualification.

Date: . . . . 2021/15/10 . . . .

i

Abstract

The role of a positive feedforward loop in regulating yeast glycolytic intermediate dynamics

S. Kotze

Department of Biochemistry,
University of Stellenbosch,
Private Bag X1, Matieland 7602, South Africa.

Thesis: MSc (Biochemistry)

December 2021

Yeast glycolysis is a well-studied model for metabolic pathways and fundamental aspects of regulation. Whereas negative feedback is common in metabolic networks; positive feedforward regulation is much less often observed. The aim of this project was to elucidate the function of feedforward loops (FFLs); investigating why they occur and to discern their potential role in disease states. A well-known FFL in glycolysis was investigated, namely that of pyruvate kinase (PK) which is known to be strongly regulated. One of its most important activators is fructose 1,6-bisphosphate (FBP), a metabolite found upstream in the pathway. Certain cancer cell lines have been shown to induce a particular isoform of PK, PKM2, which is not activated by FBP, hinting at an advantage that the absence of this FFL may confer to cancerous cells. By defining the fundamental function of FFLs, greater insights into metabolism can be obtained by investigating the effects of its absence on glycolytic flux.

To probe this question, we used a systems biology approach of experimentation in conjunction with mathematical modelling. Yeast PK was kinetically characterised using cell-free extracts and was found to be activated by FBP via an FFL and inhibited by inorganic phosphate (Pi). This kinetic data was used to analyse several PK rate equations that incorporate allosteric models

for its regulation by FBP and Pi. Based on these results a Hill-type equation was selected to extend an existing detailed kinetic model for yeast glycolysis. In addition, core model simulations were performed on systems with increasing complexity to formulate the core model hypothesis that the function of FFLs in metabolic networks is to buffer the intermediate metabolites between the regulating metabolite and regulated reaction when flux through the pathway changes, thereby preventing metabolic imbalance. We tested this hypothesis via experimental analysis of yeast glycolytic intermediates and cofactors over time after a glucose pulse to the pathway. The results showed interesting cofactor dynamics; with ATP being fully converted to AMP during glucose exhaustion and also indicated that Pi could not function as a switch-off mechanism for the FFL. These glycolytic intermediate dynamics also served as an independent experimental data-set that successfully validated the full glycolytic model that was adapted with the Hill equation to better describe PK activity and flux through the pathway as a whole.

Uittreksel

Die rol van 'n positiewe voorwaartse lus in die regulasie van gis glikolitiese intermediêre dinamika

S. Kotze

Departement Biochemie,
Universiteit van Stellenbosch,
Privaatsak X1, Matieland 7602, Suid Afrika.

Tesis: MSc (Biochemie)

Desember 2021

Gisglikolise is 'n goed bestudeerde model vir metaboliese paaie en die fundamentele aspekte van regulering. Negatiewe terugvoer is algemeen in metaboliese netwerke en is dus goed bestudeer, maar positiewe terugvoerregulering word selde waargeneem. Die doel van hierdie projek is om die funksie van positiewe voorwaartse lusse (FFLs) uit te pluis; om te ondersoek waarom dit voorkom, èn om hul potensiële rol in siektetoestande te onderskei. 'n Bekende voorwaartse lus in glikolise word ondersoek, díe van pyruvatkinase (PK), 'n ensiem wat sterk gereguleer word. Een van die belangrikste aktiveerders van PK is fruktose 1,6-bisphopshate (FBP), 'n metaboliet wat stroomop in die pad voorkom. Daar is bewys dat sekere kankersellyne 'n spesifieke isoform van PK, PKM2, uitdruk, wat nie deur FBP geaktiveer word nie. Dit dui moontlik op 'n voordeel wat die afwesigheid van die voorwaartse lus aan kankerselle kan bestee. Deur die fundamentele funksie van voorwaartse lusse te definieer kan ons beter insigte kry oor metabolisme, deur die uitwerking van die afwesigheid daarvan op glikolitiese vloed te ondersoek.

Om hierdie vraag te ondersoek, het ons 'n stelselbiologie-benadering van eksperimentering in kombinasie met wiskundige modellering gebruik. Gis-PK is kineties gekarakteriseer deur gebruik te maak van selvrye gisekstrakte en daar is bevind dat dit deur FBP via 'n FFL geaktiveer is, en deur anorga-

niese fosfaat (Pi) geïnhibeer word. Hierdie kinetiese data is toe gebruik om PK-koersvergelykings te analiseer wat allosteriese modelle inkorporeer vir die regulering van PK deur FBP en Pi. Op grond van hierdie resultate is 'n Hill-tipe vergelyking gekies om 'n bestaande gedetailleerde kinetiese model vir gisglikolise uit te brei. Verder het ons speelgoedmodelsimulasies uitgevoer op stelsels met toenemende kompleksiteit om die kernmodelhipotese te formuleer dat die funksie van FFLs in metaboliese netwerke is om die intermediêre metaboliete tussen die regulerende en gereguleerde metaboliet te buffer wanneer vloei deur die pad verander en sodoende help om metaboliese wanbalans te ontmoedig. Ons het hierdie hipotese getoets deur middel van die ontleding van gisglikolitiese tussenprodukte en ko-faktore oor tyd na 'n glukosepuls. Die eksperimente het interessante kofaktordinamika getoon met ATP wat byna ten volle omgeskakel is na AMP tydens glukose-uitputting. Met hierdie resultate het ons ook Pi uitgesluit as 'n moontlike afskakel meganisme vir die PK-FFL. Hierdie glikolitiese intermediêre dinamika het ook gedien as 'n onafhanklike eksperimentele datastel wat die volledige glikolitiese model- wat met die Hill-vergelyking aangepas is- suksesvol gevalideer het in 'n poging om PK-aktiwiteit en vloei deur die hele pad beter te beskryf.

Acknowledgements

I would like to express my deepest gratitude to the following people for enabling the completion of this project:

- My supervisor Prof. J.L Snoep for his time and support. I feel immensely fortunate to have had your expertise to guide me.

- My co-supervisor Dr. D.D van Niekerk for his guidance and careful reading.

- Dr. Theresa Kouril for her consistent help and breadth of knowledge in experimental work. Without your kind help this thesis would not have been possible.

- The Molecular Systems Biology lab in its entirety for their support. I would especially like to thank our lab manager Mr. Arrie Arends, and Klarissa Shaw for keeping everything in the MSB lab together and always being available and eager to help when something was needed.

- My parents for their continued support in all aspects of life. Every opportunity I've had I owe to you. My brother for always pushing me to be better, I'm thankful for a lifetime of healthy competition that has turned into sincere mutual encouragement over the years.

- The friends I've made in Stellenbosch over the last six years, whose companionship has been invaluable to me.

- I would like to thank the National Research Foundation (NRF) and SARChI for their financial assistance with this MSc project.

Dedications

For my mother, who raised me on books

"Choosing science doesn't mean you cannot also choose compassion, or the arts, or be awed by nature. Science is not meant to cure us of mystery, but to reinvent and reinvigorate it" - Robert M. Sapolsky

Contents

CONTENTS ix

List of Figures

List of Tables

Nomenclature

2PG	2-Phosphoglycerate
3PG	3-Phosphoglycerate
ACN	Acetonitrile
ACA	Acetaldehyde
Acetyl-CoA	Acetyl coenzyme A
ADP	Adenosine diphosphate
AK	Adenylate kinase
AMP	Adenosine monophosphate
ATP	Adenosine triphosphate
BPG	1,3-bisphosphoglycerate
CFE	Cell-free extract
DHAP	Dihydroxyacetone phosphate
DTT	Dithiothreitol
E. coli	*Escherichia coli*
ETOH	Ethanol
F26BP	Fructose 2,6-bisphosphate
F6P	Fructose 6-phosphate
FA	Formic acid
FBP	Fructose 1,6-bisphosphate
FFL	Feedforward loop
G3P	Glyceraldehyde 3-phosphate

G6P	Glucose 6-phosphate
GAPDH	Glyceraldehyde 3-phosphate dehydrogenase
GLC	Glucose
HK	Hexokinase
HPLC	High Performance Liquid Chromatography
IP-RPLC	Ion-pairing reverse phase liquid chromatography
LDH	Lactate dehydrogenase
MWC	Monod-Wyman-Changeux
NAD(H)	Nicotinamide adenine dinucleotide
ODE	Ordinary differential equation
PCA	Perchloric acid
PEP	Phosphoenolpyruvate
Pi	Inorganic phosphate
PIPES	Piperazine-N,N-bis(2-ethanesulfonic acid)
PFK	Phosphofructokinase
PK	Pyruvate kinase
PMSF	Phenylmethylsulfonyl fluoride
PYR	Pyruvate
S. cerevisiae	*Saccharomyces cerevisiae*
SAICAR	succinylaminoimidazolecarboxamide ribose-5-phosphate
TBA	Tetrabutylammonium bisulfate
TCA	Tricarboxylic acid cycle
TF	Transcription factor
YGM	Yeast growth media

Chapter 1

Introduction

Glycolysis is one of the most widely studied and characterised biochemical pathways. Due to its prevalence in almost all metabolically active cells in both prokaryotic and eukaryotic organisms, it is known to be an ancient metabolic pathway that has been conserved between species. Interest in glycolytic studies and altered glucose metabolism surged after Warburg identified increased glycolytic rates in cancer cells [1]. In the vast majority of living organisms, the glycolytic process lies at the very core of metabolism and is an integral target of both biotechnological and health studies and/or applications. Humans have also been exploiting glycolysis for centuries, and the fermentation of sugars remains a fundamental cornerstone in the food industry for many dairy, baked goods and beverage products [2]. Large strides have also recently been made in the utilisation of the glycolytic process for the production of bio-fuels [3]. Furthermore, altered glycolysis has been linked to numerous disease states such as cancer [4] and diabetes [5]. In fundamental studies of glycolysis, the aim is to increase our current understanding of glycolysis and how its components and their activities are regulated to ensure homeostasis and metabolic stability in dynamic environments. Individual glycolytic enzymes have been studied extensively in isolation; however, systems-level analyses of glycolytic flux control have not been fully explored. As such, this project aims to investigate one aspect of glycolytic regulation at a systems-level.

Glycolysis as a metabolic network consists of not only the series of reactions that converts substrate to product, but also the regulatory mechanisms that modulate the enzymes catalysing these reactions. This thesis aims to investigate an aspect of glycolytic regulation that is not yet fully explored or understood: the role of the feedforward loop (FFL) in metabolism. In contrast to the very prevalent and well-described phenomenon of feedback loops, FFLs are not as common in metabolism, and their function is not immediately obvious. In order to investigate these metabolic FFLs, the enzyme pyruvate kinase (PK), which catalyses the last step in glycolysis, will be investigated

in yeast cells. Fig 1.1 illustrates the molecular interactions of the glycolytic pathway in *Saccharomyces cerevisiae* as modelled in this study. The PK reaction results in the conversion of phosphoenolpyruvate (PEP) into pyruvate, and it is coupled with ADP phosphorylation to yield ATP. PK is known to be stimulated by fructose-1,6-bisphosphate (or FBP), which is the product of the third reaction in glycolysis. Because PK is stimulated by a metabolite found upstream in the pathway, this activation is described as a positive FFL.

Furthermore, several studies on bacterial PK have unearthed a pronounced inhibitory effect of inorganic phosphate (Pi) on PK activity, showing higher half-saturating constants for FBP in the presence of increased Pi concentrations, suggesting a regulatory relationship between the two effectors [6]. The experimental data put forth in this thesis suggests the same kinetic behaviour for yeast PK. As such, another auxiliary aspect investigated in this project is the inhibitory effect of Pi on PK, and the potential role it plays in the PK-FFL. We postulate that it can function as an "off-switch" for the PK-FFL, allowing us to experimentally investigate how glycolysis changes when the FFL is inhibited. Fig 1.2 shows the three-noded PK-FFL. The nodes represent either metabolites (FBP and PEP) or enzymes (PK), and the edges represent reactions. Intermediary reactions may occur between the regulating and regulated node, as in the PK-FFL, where several reactions take place between FBP synthesis and PEP conversion by PK.

The research question this thesis aims to address is: Can the purpose of a positive feedforward loop in metabolism be understood in generic terms? To investigate this question, we used a systems biology approach to study the PK-FFL in yeast and how it regulates glycolytic intermediate dynamics. As such, our approach was two-pronged: A combination of experimental work and mathematical modelling was used to probe the FFL mechanism. With regards to the mathematical modelling aspect of this project, we analysed simple core models to formulate a core model hypothesis, and used a Hill-type PK rate equation to adapt an existing yeast glycolytic model. Experiments were performed to obtain fitted kinetic parameters for the new PK equation, which is then incorporated into the full model which we aimed to validate with experimental time-course data.

Chapter 2 of this thesis is a brief overview of the relevant literature on glycolytic regulation, regulatory loops, known FFLs and the regulation of PK in yeast and other cell lines. Chapter 3 outlines the results of the first objective of this project, which was the kinetic characterisation of PK using *S. cerevisiae* extracts, in particular with regards to the respective activating and inhibitory effects of FBP and Pi. Chapter 4 addresses the second objective, which was to use the kinetic data obtained to perform a comparative analysis of novel PK rate equations derived from allosteric models, which include terms for the
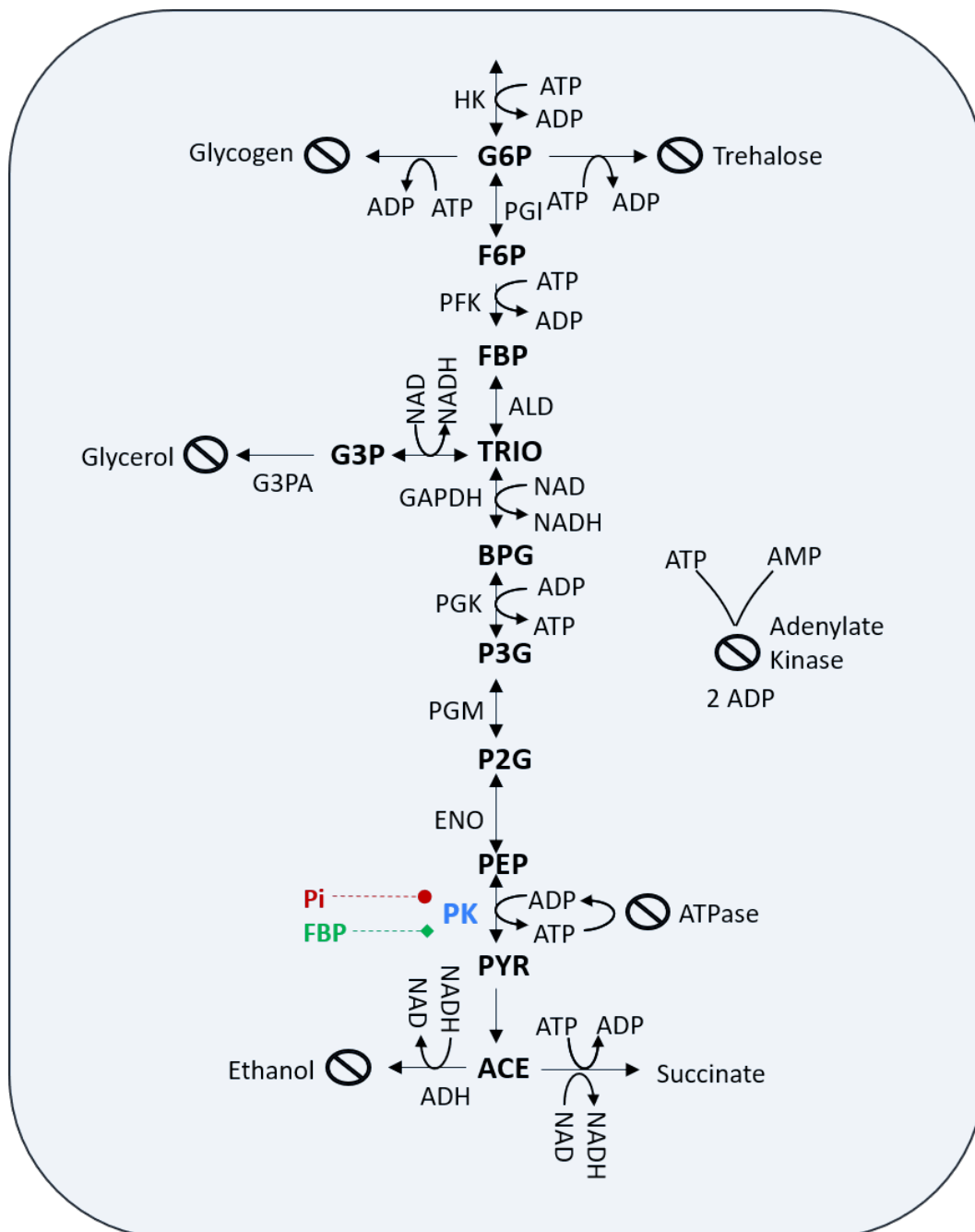
Figure 1.1: A scheme of the model showing the molecular interactions of the glycolysis pathway in *S. cerevisiae* strain X2180. The enzyme of particular interest in this study, pyruvate kinase (PK) is shown in blue. Regulation of PK is indicated by dashed arrows; with allosteric activation by FBP depicted in green (signifying the feedforward loop under investigation), and inhibition by Pi in red.
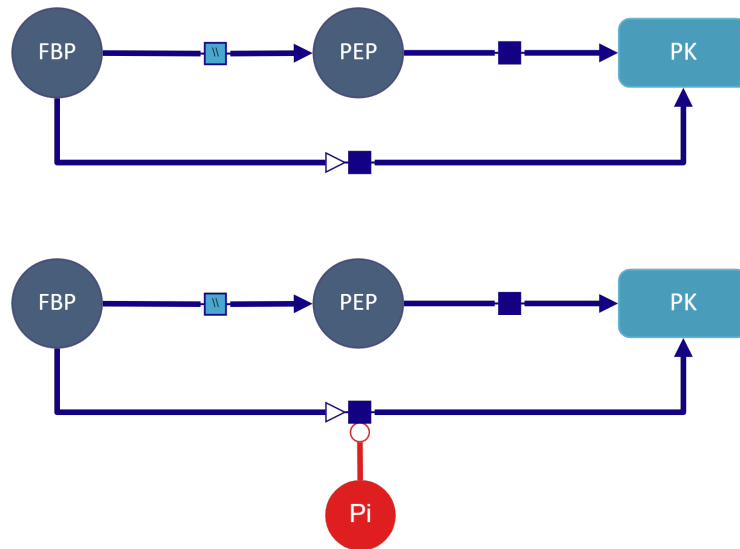
Figure 1.2: The PK-FFL illustrated with its activating effector, FBP. The bottom panel shows the proposed inhibitory effect of inorganic phosphate (Pi) on the PK-FFL.

observed regulatory effects of FBP and Pi on PK, and to obtain new parameter estimates for PK. Chapter 5 outlines the results of the third objective, which was to formulate a preliminary core model hypothesis for the general function of FFLs in metabolic systems by setting up four minimal core model systems, simulating the effects of an FFL and comparing them to the same systems without a FFL. Chapter 6 addresses the fourth objective, where we aim to illustrate the core model hypothesis for a real metabolic system, and outlines the results of experiments investigating the glycolytic intermediate dynamics of yeast after a glucose pulse to the pathway in the presence and absence of Pi, as a proposed "off-switch" for the FFL. The fifth and final objective also addressed in Chapter 6 was to validate the altered glycolytic model with the novel PK equation using an independent set of time-course data for glycolytic intermediates. Chapter 7 provides a general discussion and summary of the findings presented in this thesis, as well as recommendations for future work.

Chapter 2

Background

2.1   Glycolysis

The Embden-Meyerhof-Parnas pathway for glycolysis is a linear series of ten enzyme-catalysed reactions that converts glucose into two molecules of pyruvate, with ATP and NADH being formed by the free energy released [7]. The reactions take place in the cytoplasm and are anaerobic. The intermediates formed through these reactions can be funnelled off to various other pathways in order to produce biomass in the form of proteins, lipids or nucleic acids. Even though glycolysis is a process common to most organisms, the fate of its end-product, pyruvate, is varied and dependent on the type of organism or tissue. In cells that lack mitochondria (such as erythrocytes), or cells that contain mitochondria but with limited oxygen supply (such as muscle cells during exercise), anaerobic glycolysis occurs, otherwise known as fermentation [8]. Depending on the cell type, the pyruvate is reduced and thus fermented to products such as lactate, ethanol or acetic acid. In contrast, in the presence of oxygen, cells containing mitochondria transport the pyruvate into the mitochondria where it is oxidised to acetyl coenzyme A (Acetyl-CoA) which then passes on to the tricarboxylic acid (TCA) cycle to be metabolised into carbon dioxide (CO_2) and water, generating far greater amounts of ATP [9]. Thus, glycolysis occurs under both aerobic and anaerobic conditions, with the pathway being exactly the same in both instances, except for the end product formed and the ultimate energy yield.

The glycolytic pathway can be divided into two smaller sections, namely lower and upper glycolysis. Upper glycolysis, also known as the preparatory phase, consists of the first five reactions and requires ATP to convert glucose into triose-phosphates. In contrast, lower glycolysis comprises the final five reactions and produces ATP by converting triose-phosphates into pyruvate, as such it is also known as the pay-off phase [8]. In total, 2 ATPs are consumed and 4 ATPs produced, making the net energy product of glycolysis 2

molecules of ATP per glucose converted [10]. Glycolysis can be considered as performing two major roles: I) energy production and II) the formation of biosynthetic precursors that are utilised by different metabolic pathways for biomass production, metabolic stress protectants and secondary products such as hormones [11, 2].

Control of the glycolytic flux is important as it contributes to circulating glucose homeostasis and provides energy or biomass precursors vital for cell proliferation. It has also been found that the flux through glycolysis is linked to the concentrations of glycolytic intermediates that are sensed by various cellular processes [12]. Indeed, the regulation of glycolysis is so integral to cellular function that glycolytic dysregulation has been linked definitively to numerous disorders. As will become evident, no consensus has yet been reached on which enzymes, effectors, metabolites or external conditions contribute most to glycolytic regulation. Considering the recent implication of glycolysis in some of the most pertinent diseases facing humanity today and its long-standing importance for food security and alternative fuels, the continued interest in glycolytic studies 80 years after it was first described comes as no big surprise.

As long as a functional description of its multi-layered regulation (which includes changes in gene expression, post-translational modifications, and allosteric interaction) eludes us, the impetus for glycolytic studies remains, such that we can learn to successfully intervene and manipulate the behaviour of the pathway. The next section will explore regulation, how it contributes to homeostasis and why it is important to include all its facets into glycolytic models.

2.2 Regulation and control of glycolysis

First, it is important to distinguish the difference between control and regulation within the context of a systems biology view of metabolism. These two terms are often used interchangeably, however a nuanced distinction has been made by Sauro [13] who defines control as the ability to direct behaviour, and regulation as the process which allows control to be achieved. Practically speaking, in Metabolic Control Analysis (MCA), control refers to the ability to change a flux or concentration, and regulation is the mechanism through which homeostasis is achieved, i.e to resist changes [14].

Although the basic functions of glycolysis (such as the production of energy equivalents and biosynthetic precursors) are conserved amongst species, the environment in which it occurs can vary greatly amongst tissues and species. Fluctuations in external environmental dynamics necessitate that the enzymes involved regulate glycolytic flux such that the right products are provided at the appropriate time in the appropriate quantities. Due to this, organisms

and tissues have formed fine-tuned, multi-level systems that control metabolic flux over both short and long periods of time [2]. As such, the kinetic properties of enzymes differ amongst species, which affords flexibility and enables different organisms and tissues to adapt the glycolytic process according to their unique needs. Furthermore, regulation of metabolism is also important to prevent futile cycling. Many pathways in metabolism are reversible, and so can proceed in both the forward and reverse direction. To prevent futile cycling of a metabolite like ATP it is important that a pathway does not proceed in both directions at the same time. To prevent this, enzymes of opposing, non-equilibrium reactions must be regulated reciprocally. As such, the specific activity of an enzyme in one pathway is activated whilst the specific activity of an enzyme in the opposing pathway is simultaneously inhibited, often using the same mechanism (e.g., binding of the same allosteric regulator or using the same covalent modification which results in opposite effects). Partial futile cycling, however, is a valuable tool in regulation as there can be greater control of flux if two opposing pathways occur at the same time [15].

The simplest view of the control of metabolic flux can broadly be divided into two categories: The control of I) substrate availability and II) enzyme activity. Broadly viewed, enzyme activity can be modulated by changes in the amount of enzyme present due to the processes of synthesis and degradation, the type of enzyme by the expression of different isozymes that differ in catalytic activity, and lastly the specific enzyme activity. The regulation of specific enzyme activity is a major mechanism to control metabolic rates and is brought about mainly by allostery and covalent modification. The outermost layer of regulation involves hormones and extracellular signals that allows communication between tissues and cells. For example, the hormone insulin is known to promote glycolysis, whereas glucagon has the reverse effect [16]. Hormone signals are considered long-term modulators as their influence cannot be seen on a second or minute timescale. As such, these will not be discussed in great detail in this study, but it is worth keeping in mind the many layers of regulation as metabolic needs may fluctuate in a manner of seconds or over prolonged periods. Metabolic responses to changes in the environment may occur in seconds, far more rapidly than the information in DNA can be read and applied. As such, enzymes may be allosterically activated or inhibited by non-covalent interactions with small molecules called effectors, modulators or allosteric regulators which regulate metabolic flux on a millisecond to minute timescale and this is the chief concern of this study. The collective purpose of all these processes is to funnel metabolites through biochemical pathways at levels required by cells or tissue depending on their function and their dynamic environment.

The flow of carbon metabolites through the pathway is defined as the glycolytic flux. Eric Newsholme in the 1970's was one of the first to describe

the behaviour of non-equilibrium, near-equilibrium and steady-state reactions in the context of flux control through metabolic pathways [17]. He postulated that due to the fundamental thermodynamic structure of biochemical pathways, they can be controlled at non-equilibrium steps by effectors and covalent modifications [18]. Non-equilibrium reactions are known to be essentially irreversible under physiological conditions as there is a negative free energy change at these steps that may be lost as heat or transferred to another molecule (for example the formation of energy-rich phosphate bonds). Because of this, irreversible reactions within biochemical pathways such as glycolysis are described as "committed steps", or flux-generating steps. The movement of the flux of metabolites through irreversible reactions results in heat, products and intermediates that are needed for the maintenance of cellular function. As such, individual tissues or cells contain the appropriate levels of enzymes and metabolites needed to steer the flux in the pathway towards a particular product at required levels to serve a physiological function [19]. Newsholme's studies illustrated that metabolic pathways contain multiple steps, all under coordinated regulation which resulted in the description of these pathways as a series of enzyme-catalysed reactions which is initiated with a flux-generating step and ends with a reaction preceding another pathway (i.e. another flux-generating step), or loss of product. With this principle as a guide, the equilibrium and non-equilibrium reactions of several metabolic pathways were determined experimentally. With the identification of non-equilibrium reactions and the flux-generating steps, researchers determined the key regulatory reactions and the key enzymes that catalyse them. According to these principles, the classic view of glycolytic regulation was established: The three virtually irreversible reactions HK, PFK and PK were identified as the key steps [18, 11]. The activities of these key enzymes are regulated by one or more of the mechanisms described above, such as reversible binding of allosteric effectors or by covalent modifications such as phosphorylation. Additionally, the dynamic metabolic needs dictate the rate of transcription to regulate the levels of these key enzymes.

However, many studies since have sought to dispel this simplistic view and have argued that other factors may play a more significant role. For example, Tanner *et al* insisted that enzymes in lower glycolysis such as PK do not exert significant flux control. He concedes that the two committed phosphorylation steps PFK and HK are indeed significant flux-controlling steps, but that the rest of the control lies with glucose import and product export [11]. Another recent study by van Heerden *et al* [15] argues that the over-expression of glycolytic enzymes does not result in increased flux through the pathway and argues that glycolytic flux control lies outside of the pathway itself. He posits that two factors play a role, the first being glucose import which controls flux only when supply is limiting. According to this study the second and most significant factor that regulates glycolytic flux is ATP demand. True to

supply-demand logic as laid out by Hofmeyr [20], a surplus of ATP inhibits several glycolytic enzymes and thus ATP supply. However, he postulates that PFK is the primary regulatory target of ATP demand, as it is insensitive to its product yet sensitive to ATP. As such, the flux is controlled by PFK not based on its product, but instead on ATP demand which exerts global control as varying ATP levels dictates ATP synthesis via glycolysis by acting on PFK [2]. The importance of the ATP/AMP ratio is also frequently cited, since ATP allosterically inhibits key enzymes such as PFK, whereas AMP reverses this effect [9, 21]. Since AMP is the signal for the low-energy state, enzymatic activity increases with a lower ATP/AMP ratio, meaning that glycolysis is stimulated as a result of a drop in energy charge [7].

Among the dissenters to the classic view of regulation was an early group that was opposed even to the notion of relegating certain enzymes in a network as rate-limiting and the use of terms such as "pacemakers" and "key regulators". In two independent seminal papers, Kacser and Burns [22] as well as Heinrich and Rapoport [23] lay the foundations for MCA, which sought to dispel the reductionist approach of hunting for rate-limiting steps within pathways, arguments which they saw as fruitless. In metabolic steady-state under which these pathways are studied, all reactions along a linear pathway by definition have the same rate, so in principle when one tries to identify the "slowest" step along a pathway, it is the one least able to go faster. Another way of framing it would be to say it is the step which would result in the greatest change in flux throughout the pathway as a whole if its rate was varied. Classic biochemical observation of enzymes in isolation, removed from its physiological context, seemed to be poorly equipped to deal with the issue of identifying this step. As stated before, when the activity of the supposed rate-limiting enzymes was varied experimentally, the significant changes in flux through the pathway one would expect within this paradigm was simply not observed. Thus, early evidence showed that flux through even the simplest pathways is most probably dependent on the rate constants of several of its constituent reactions, and that a new approach would be needed to tackle the issue of metabolic control [24]. Apart from MCA, two other approaches were being developed to address this issue: a flux-orientated approach by Crabtree and Newsholme [25, 26], and biochemical systems theory by Savageau [27]. Though a contentious debate during the conception of this field, the arguments of which theoretical framework is most appropriate for studying real systems was put to rest by a study that proved that in essence, all three theories reach the end by different means [28]. However, MCA has enjoyed greater popularity and longevity as the field of metabolic control matures, and is arguably the most important theoretical framework in the system biologist's toolkit today for analysing metabolic networks and regulation. Whatever their differences, these approaches fundamentally re-framed the question of control from qualitative to quantitative. That is, from asking *whether* a step is rate-

limiting or not, to being able to assign a value to *how much* metabolic flux changes as the enzyme activity varies. In so doing, MCA subverted the widely accepted view that the degree of displacement of a reaction from equilibrium necessarily correlates with its degree of control of flux. These theories formed part of the first steps towards a systems view of biochemical reactions (an approach which is explored more fully in the final section of this chapter), and formed a more secure theoretical base for the analysis of the kinetic behaviour of metabolic pathways.

The purpose of this study is not to elucidate which mechanisms or steps are most important for the regulation of glycolysis, but rather to establish the role of FFLs within the context of metabolic regulation as a whole. However, it is useful to remember that whatever the extent of the importance of these loops, they form part of an intricate system with multiple components that are in constant communication with one another to ensure cellular needs are met in terms of energy production and biosynthetic precursors, without any waste. Within the scope of the regulation mechanisms outlined above, metabolic loops form part of allosteric regulation as they usually involve intermediate metabolites from a pathway that act as effectors to enhance or inhibit enzymatic activity within the same pathway. The next section will explore the significance and prevalence of regulatory loops in biological networks such as metabolism and gene expression in order to elucidate a possible common cellular need that gives rise to these patterns.

2.3   Network motifs within biological networks

Glycolysis is considered a metabolic pathway because it consists of a chain of enzymes that converts a substrate to a product with a series of intermediate steps. However, like most metabolic pathways, glycolysis does not function in isolation, as many other pathways (such as the Pentose Phosphate Pathway, TCA cycle *etc*) share the same intermediates [7]. As such, these pathways are connected in such a way that they become interdependent on one another. Because of this, metabolism can be described as a network, which is in actual fact a sub-network of the global network of the cell [29]. The metabolic network consists not only of the reactions that comprise metabolism and whole metabolic pathways, but also the regulatory mechanisms that modulate the enzymes catalysing these reactions. The rise of systems biology has enabled scientists to abandon the reductionist approach of viewing enzymes in isolation. Instead, metabolism can now be thought of in terms of networks, allowing for flexibility, since the network is continuously reconfigured at the behest of changing environmental conditions and physiological needs [30]. Viewing metabolic pathways as a network allows us to consider metabolites and enzymes as nodes and the reactions connecting them as edges [31].

Since glycolysis can be viewed as a network at systems level, it has been discovered that it adheres to properties typical of these diagrams. Within the larger network, sub-graphs known as network motifs have also been identified [32]. Network motifs are recurring patterns found in almost all types of networks [16]. These patterns are identified by comparison with randomised networks that are comprised of the same number of nodes and edges as the real network, but which have random linkages between metabolites. Patterns that are found more frequently in real networks than in randomised networks are considered meaningful since they have been selected for over an evolutionary timescale and thus confer some kind of advantage [31]. When one considers that a single mutation can result in either the loss or addition of an edge due to the disruption or creation of a binding site, as well as the frequency with which mutations occur (especially in a rapidly proliferating organism such as yeast), it follows that under such forces of randomisation, any pattern of edges which persists in biological networks over vast amounts of time and across several types of organisms must be selected for.

It has been established how glycolysis can be considered as a network, however, there are several other types of biological networks which all share these motifs. The most notable and well-studied of these is the gene transcription network. Extensive experimental and theoretical studies have been done to identify network motifs in physiological circuits and to discern their unique contributions and how each arises specifically to fulfil an advantageous function. A vast body of work by Uri Alon lays out these circuits in terms of the design principles they share and describes how these principles form the basis of systems biology [31]. However, the bulk of his work is focused on gene transcription networks, and although some similarities between transcription networks and metabolic networks may exist, it cannot be presumed that the function of any network motif will serve the same purpose in these distinct circuits. Metabolic networks differ from transcription networks in several fundamental ways, most notably by the properties of their respective nodes. In transcription networks the nodes are genes, which act vastly different from their counterpart in metabolic networks, which can be metabolites, regulators or enzymes [33]. For example, many network motifs described by Alon serves a primarily time-sensitive response, providing an advantageous delay in the activation or deactivation of gene transcription as defined by the cellular needs that gave rise to the motif. Indeed, Alon stresses the importance of taking time-frames into account when setting out to elucidate how a network motif affects network dynamics, since the functions of gene transcription networks are almost entirely inferred from the separation of timescales between binding of transcription factors (TF) and protein accumulation. With Alon's description of these networks, TF levels can be assumed to be at steady state within a mathematical description of the entire network because the binding of the TF to its DNA site reaches equilibrium in a matter of seconds, whereas

the accumulation of the transcribed protein product takes several minutes to hours. Pivotal as these considerations are in gene transcription networks, the same assumptions would not necessarily be applicable in metabolic networks. An important distinction is that there is no flow of mass in gene transcription networks as there is in metabolism, and they also tend to operate on a slower timescale.

However, these differences in spatial and temporal reactions of various networks to their built-in motifs merely serve to illustrate the extensive and varying functions they may serve depending on where they are found. It remains true that these motifs are common to a vast array of networks. Within living organisms network motifs have been identified in gene transcription, metabolic, developmental, and neuronal networks; as well as in signal transduction and protein circuits found in processes such as bacterial chemotaxis [31]. When one speaks of a network motif as a pattern, one refers to the configuration of the nodes and edges comprising this section of the network. This includes the number of nodes and edges involved, as well as their relationship to one another. In other words, this "sub-graph" is merely a selection of particular nodes and their edges exhibiting network motif behaviour within the larger frame of the complete network. For example, a metabolic network such as glycolysis may be comprised of numerous metabolites and enzymes (nodes) all participating in one or many reactions (edges), however when isolating a network motif, it involves only the metabolites directly involved in the motif, regardless of whether other intermediates are present between the nodes of interest [34].

As such, network motifs are usually classified according to the number of nodes they are comprised of. This is because the function of the motif is dictated and limited by the number of genes or metabolites involved. Another important factor for classification is the edge interaction with the nodes, and also the sign of the edge. The sign of the edge refers to the effect it has on the node. Within the gene transcription framework, activation (positive control) occurs when the binding of the effector increases the activity of the enzyme. Conversely, inhibition (negative control), is brought about when the binding of the effector decreases enzyme activity [31]. Similarly, in metabolic networks, any reaction defined as an edge in a network motif serves to either increase or decrease the levels of the metabolites involved and is therefore classified as a positive or negative edge, respectively. Since most metabolic reactions are reversible, it has been more commonly proposed to define the connecting reactions as reversible edges, though it is often useful to simplify the motif for analysis by defining the edge sign by the reactions prevailing equilibrium as found *in vivo*. For example, since the final reaction in glycolysis catalysed by PK is virtually irreversible, one considers the edge to be positive (towards the production of pyruvate).

As the entire metabolic network of the cell is too complicated to analyse, it is necessary to restrict attention to specific sub-systems within the larger network. A review of the literature on biological networks emphasises the importance of studying cellular pathways as a network due to their highly interconnected nature, as opposed to merely studying them as discrete reactions in isolation. This provides a framework for local analysis of the dynamic properties of these networks as brought about by motifs that result in specific, modular functions [34]. The most common of these recurring patterns fall within three broad classes as shown in Fig 2.1: Auto-regulation, simple regulation, and regulatory loops [35]. Auto-regulation, or auto-catalysis, consist of only one node and one edge, and can be further split into negative or positive auto-regulation depending on the sign of the edge, in other words, whether the metabolite inhibits or activates its own synthesis. Simple regulation, which consists of two nodes connected by one edge is simply when one metabolite activates or inhibits the synthesis of another. However, our interest lies primarily with regulatory loops, which are characterised by having three nodes and three edges. This category of network motif can further be split up into feedforward and feedback loops, which will be explored in greater detail in the following section.
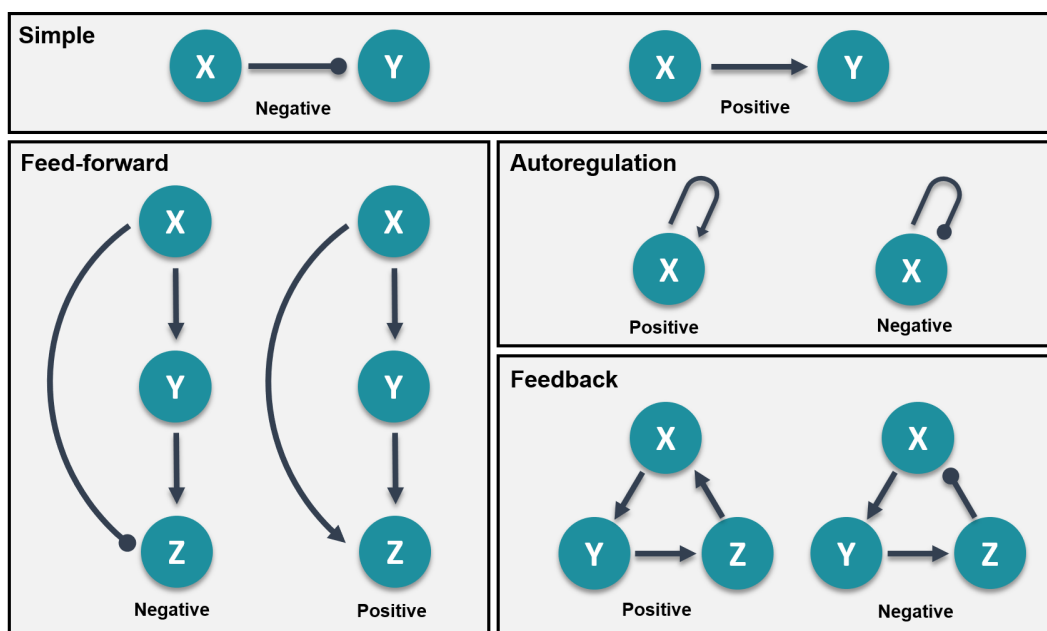
Figure 2.1: Common categories of network motifs as can be found in most networks such as glycolysis. Simple regulation occurs when one metabolite regulates the synthesis of another. Auto-regulation entails a single metabolite regulating itself. Three-noded motifs are known as regulatory loops and are comprised of feedback and feed-forward activation or inhibition. Positive regulation i.e., activation denoted by ▲, negative regulation i.e., inhibition denoted by ●.

2.4   Regulatory loops: Feedback and feedforward

The literature on regulatory loops within the context of gene transcription is extensive. However, as mentioned before these elucidations of mechanics and function with transcription networks cannot be directly transposed onto metabolic networks, and there is a dearth in the literature on what purpose the FFL serves in metabolism specifically and how its structural properties allow them to fulfil it. As such, detailed descriptions of several regulatory loop sub-types and their functions within gene transcription networks can be found elsewhere [31], and this section concerns itself with reviewing the available literature on these loops specifically within the context of metabolic networks such as glycolysis.

The two broad classes of regulatory loops are feedback and feedforward loops. Feedback loops are prevalent in metabolism and as such have been the focus of many studies in an attempt to capture their mechanisms of action, origin and effects. Such studies have ascribed numerous biological functions to feedback designs, such as signal amplification and bi-stability for positive feedback; robustness and homeostasis for negative feedback; and polarisation or oscillations for mixed feedback motifs [36, 34, 37]. Some well-known examples of negative feedback within glycolysis specifically include the inhibition of PFK by citrate and ATP, so that enhanced TCA cycle activity which produce these products provides negatives feedback which inhibits PFK and glycolysis. For more examples, a recent review by Locasale explores the numerous known feedback loops found within the regulation of glucose metabolism [12].

FFLs, however, are not as common and do not make as much intuitive sense within a homeostatic framework. The uncertainty surrounding their exact role within glycolytic regulation is the focus of this thesis. Though FFLs are slightly more obscure than feedback loops, some known examples can be found within metabolism. The activation of L-LDH by FBP in lactic acid bacteria is an example of a glycolytic FFL that has garnered more attention in recent years [38, 39]. One of the older examples of positive feedforward simulation is that of PFK. Fructose 2,6-bisphosphate (F26BP), which is synthesised from PFK's substrate F6P had been found to be a strong activator of PFK. Thus, when glucose increases, the resulting abundance of F6P stimulates the production of F26BP, which in turn stimulates PFK [7]. More examples of such feedforward loops within and outside of central metabolism are known [40]. It is interesting to note that in many of the above examples of metabolic FFLs found in various different organisms, whatever the enzymatic target, FBP and its derivatives seem to be a recurring activator within FFLs. Similarly, PK, as the focus of this study, has been proven to be activated by FBP via an FFL in yeast. However, it is interesting to note that even in organisms and tissue types

where FBP is not the activator, PK is often stimulated via an FFL by some other intermediary metabolite. The stimulation of several isoforms of PK via feedforward activation is explored in greater depth in the following section.

2.5   Pyruvate kinase

PK facilitates the 10th and final step in glycolysis, whereby the transfer of a high-energy phosphoryl group from PEP to ADP yields pyruvate and ATP.

$$PEP + ADP \Longleftrightarrow \text{pyruvate} + ATP \tag{2.5.1}$$

PK requires the monovalent cation K^+ and the divalent cation Mg^{2+} for its activity. The reaction has a very large K_{eq} in the range of $10^3 - 10^4$ and is thus virtually irreversible under physiological conditions. Due to the irreversible nature of the reaction, it has classically been viewed to be a critical control point of metabolic flux in lower glycolysis as mentioned in earlier sections. PK is a homotetrameric enzyme with identical sub-units and responds to the cellular energy state by transitioning between tense (T) and relaxed (R) states, thereby regulating glycolytic flux [41].

In all three domains of life, PKs generate ATP in the ultimate step of glycolysis. Most PKs found in bacteria and eukarya are allosteric enzymes that are activated by sugar phosphates [42]. FBP is the most common effector, however, the activating metabolite varies across several organisms. F26BP, ribose 5-phosphate and G6P have all been identified as specific feedforward activating effectors of some bacterial PKs [43]. AMP, considered a sugar phosphate due to its phosphorylated ribosyl moeiety and the fact that it binds to the same allosteric site as other sugar phosphates, is also a common general regulator which acts largely in response to changes in cellular energy. Archaea utilise slightly more unusual glycolytic pathways, but a recent study has found that many PKs from the species in this domain is allosterically activated by 3PG generated in an irreversible reaction in the altered glycolytic pathway of these archaea, and thus it also functions as a feedforward regulator [44]. It has been proposed that the PK substrate PEP and the activating sugar phosphate (such as FBP), cooperate to shift equilibrium towards the R state, while classic inhibitors such as ATP and Pi favour the T state [45].

In mammalian cells, four PK isoforms have been identified: The L, R, M1 and M2 isozymes. The prevalence of a specific PK isoform in any given tissue depends largely on its metabolic requirements. The R isoform is expressed in erythrocytes. The L isoform is predominant in gluconeogenic tissues such as the liver [46]. PKM2 is expressed in the kidneys and lungs, and is the

predominant isoform in proliferating cells such as embryonic and tumour cells. The PKM1 isoform has been documented as being locked in the R-state, and is often described as a constitutively active splice-variant of PKM2 [41, 47]. Due to its high activity, it is found in adult skeletal muscle, brain and heart-tissues which all require ample supplies of ATP. PKM1 is the only isozyme that exhibits hyperbolic kinetics and is not allosterically activated by a sugar phosphate via an FFL.

PKM2 is an interesting PK isoform due to its strong association with tumour growth. PKM2 is the predominant PK isoform in cancer cells and exhibits lower catalytic activity than its splice-variant PKM1, but is heavily regulated to allow for metabolic flexibility and to aid with cellular adaptation to changing environmental conditions [48]. It has been found that PKM2 can shift glucose metabolism in favour of cancer cell proliferation, as it is a key regulator of the glycolytic intermediates and their metabolic fate. One study reported that decreased PKM2 activity leads to an accumulation of the glycolytic intermediates above the PK reaction, which means that they are more readily available to be used as precursors for biosynthetic processes coupled to glycolysis [49]. An example of this was a study that investigated a potential link between the glycolytic and serine biosynthesis pathways, as both have been proven to be crucial for cancer cell survival. If PKM2 is preferentially expressed (as it is in cancer cells) overall PK activity drops and there is a resultant accumulation of glycolytic intermediates which are then funneled into the serine synthesis pathway. This is significant because they found that depending on the properties of the binding site, PKM2 is independently allosterically activated by either FBP or serine [50]. A further study showed that a certain intermediate of purine nucleotide biosynthesis called SAICAR (succinylaminoimidazolecarboxamide ribose- 5'-phosphate), which is another metabolite that is abundant in proliferating cells, also activates PKM2 [51] and promotes cancer cell survival when nutrients are limited [52]. Both the serine and SAICAR biosynthetic pathways shoot off from metabolites found upstream from PK in glycolysis (3PG and G6P, respectively) [53], and it is intriguing to suppose that these molecules act as independent effectors in additional FFL loops that come into play when reduced PK activity results in intermediate accumulation. Indeed, one study posits that it is erroneous to view PKM2 merely as a constitutively inactive PK isoform, but rather as one that can be specifically stimulated by ligands as dictated by cellular needs [54]. As such, it is perhaps inaccurate to label PKM2 as inherently oncogenic, as it would be more appropriate to associate low PK activity in general with tumorigenicity [55].

The prevailing view at this point is that reduced PK activity creates a bottleneck at the terminal end of glycolysis which is critical for tumour growth, as it promotes anabolic metabolism and cell proliferation through the accu-
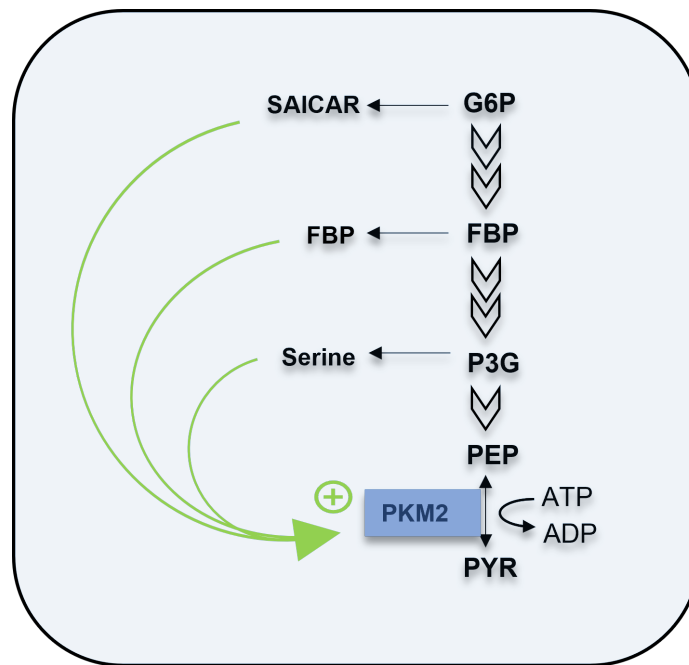
Figure 2.2: The PK-FFL illustrated with its most common activating effector, FBP. The nodes in metabolic networks can be metabolites (FBP and PEP) or enzymes (PK).

mulation of glycolytic intermediates [47]. It plays a significant role in altered cellular metabolism and it has been proven that the switch from the adult M1 PK isozyme to the M2 splice-variant in tumor cells is responsible for these cells expressing the metabolic phenomenon known as the Warburg effect [56]. Indeed, replacing PKM2 with other more active PK isoforms has been shown to reduce abnormal cellular metabolism [51].

The most important difference between the PKM1 and PKM2 two isoforms lies in the fact that PKM2 is stimulated by FBP via an FFL, whereas PKM1 is not [57]. The constitutively active PKM1 exhibits much higher activity than PKM2, which requires FBP stimulation to reach its maximal activity levels. Notably, when PKM2 is inhibited, PEP levels subsequently rise which has been found to inhibit PFK-2 in certain cell lines. F26BP (a well-known activator of PFK) levels consequently drop as PFK-2 is responsible for its synthesis, leading in turn to decreased FBP concentrations. Studies have shown that cells which predominantly express PKM2 have lower overall fructose-bisphosphate levels when compared to PKM1 cells, which exacerbates the already low PK activity in these cells, as there is now also less of its allosteric activator FBP to bolster PK activity [56].

The splice-variants PKM1 and PKM2 in mammalian cells are by no means an exception. Research into the isozymes specific to several classes of other

organisms continue to reveal the presence of PK isoforms that differ specifically with regards to whether they are sensitive to the feedforward activator FBP (or any other sugar phosphate fulfilling the same role). For example, *Escherichia coli* PK was also found to be activated by FBP [58]. However, further studies revealed that two PK isoforms exist in *E. coli*, one that is sensitive to FBP, and one that is not [59]. A study by Boles *et al* revealed that yeast cells too encode a second functional PK isozyme that is catalytically insensitive to FBP [43]. They propose that the expression of this unregulated PK isoform is de-repressed only when glycolytic flux is low and intracellular FBP levels are not sufficiently high enough to activate the normal PK variant. This trend in the variable expression of PK isoforms that are either regulated via an FFL or not hints that the FFL serves a very specific, evolutionary purpose. Furthermore, the persistent prevalence of a FFL that activates PK across most living organisms speaks to the importance of this network motif for central cellular metabolism. The following section will look more closely at the PK-FFL specifically and the varying theories that have been put forth to date to explain its significance, as well as the potential role of Pi in the PK-FFL.

2.6 The PK-FFL

The background given in the preceding sections of this literature review aims to highlight the importance of the regulation of PK within the context of glycolytic flux control. As is evident, glycolysis itself as a metabolic process is fairly well-conserved between organisms, from the simplest bacteria to man. Therefore, so too are its constituent enzymes and the mechanisms by which they are regulated. The overarching aim of a systems biology approach is to understand the properties of a system such as glycolysis or cellular metabolism, which emerges from the interaction of its well-characterised parts. *S. cerevisiae*, as one of the simplest eukaryotic organisms that derives its energy from glycolysis, is one of the most important model organisms for studying biochemical pathways and genes. Many gene sequences are highly conserved and encode for similar proteins in mammals. Systems modelling has enabled methods of investigating the interactions among various active components of the cell, and comparative analysis of these pathways has shown that substantial homology exists between the functional pathways of humans and yeast, including the cell cycle and central metabolism, and thus glycolysis. Indeed, these conserved biochemical pathways were originally identified and characterised in yeast. Because of this, *S. cerevisiae* is used in this study as a model organism to study the role of a positive FFL in regulating glycolytic intermediate dynamics.

As explored previously in this text, PK has risen and fallen in estimations of importance for glycolytic flux control over the years. As the catalyst of one

of the three virtually irreversible reactions of glycolysis, PK had initially been considered a rate-limiting step and a critical point of glycolytic flux control. Later studies disputed this view [56, 11]. It does not seem that consensus has yet been reached as to a definitive description of PK's exact role and how its regulation allows the fulfillment of that role. This is not surprising considering the multiple facets and layers of hierarchical regulation which confounds a simple description. However, the allosteric activation of PK by FBP via an FFL has garnered some interest over the years, and as far as is evident, three theories have been put forth as to its significance.

The first theory is based on PK's implication in yeast's ability to switch rapidly between respiratory and fermentative glucose metabolism in response to changing oxygen and sugar levels. *S. cerevisiae* exhibits remarkable metabolic flexibility in response to fluctuating substrate levels. It has been proven that a rapid switch to fermentative metabolism upon glucose addition is initially facilitated entirely through changing levels of the substrates, products and effectors of glycolysis. A systems level study that calculated metabolic coefficients established that regulation was entirely dominated by metabolic regulation in the first 45 minutes after switching to fermentative conditions. It was only after this initial period that transcription, translation and post-translational modification came into play [60]. Once it had been established that metabolic regulation was almost exclusively responsible for the rapid shift between glycolysis and gluconeogenesis, PK had once again been singled out as one of the key enzymes whose regulation by these glycolytic metabolites and effectors was crucial for the switch. It has been found that even though yeast PK is covalently modified in response to glucose addition, allosteric regulation is solely responsible for the control of PK activity. As such, this allostery allows switch-like rapid activation and inhibition of PK upon glucose addition and removal, respectively. Thus, not only is PK regulation central to the switch between gluconeogenesis and glycolysis, but the activation of PK by FBP results in metabolic flux being controlled exclusively by enzymes and core metabolites. This once again speaks to the presence of intrinsic metabolic regulation, which does not rely on other methods of regulation such as transcription, covalent modification or signalling by small molecules [61]. The first theory thus propounds that the PK-FFL mechanism allows cells to sense changes in glucose availability by increasing glycolytic rate [15]. Gluconeogenic growth is also associated with low FBP concentrations, which consequently results in low PK activity. As such, it has been postulated that the positive control of PK by FBP prevents futile cycling during gluconeogenesis and provides the mechanism for switching between glycolysis and gluconeogenesis so that these two opposing pathways are not operating simultaneously. When glucose is in excess, PK activity needs to be high enough to supply ample amounts of pyruvate and ATP. But under gluconeogenic conditions when glucose availability drops, it is required for PK activity to be down-regulated to avoid futile cycling

between pyruvate and PEP [43].

The second theory proposes that the FF activation of PK by FBP ensures robustness to rapid changes in substrate availability through the maintenance of sufficient PEP levels, which is needed for sugar uptake and phosphorylation in organisms that use the phosphotransferase system for glucose uptake [62]. It is postulated that the PK-FFL prevents an irreversible metabolic collapse during sporadic periods of starvation by introducing a "safety valve" that regulates the utilisation of PEP by PK based on glucose availability. FBP activation and Pi inhibition of PK, as well as the regulation of PFK by PEP, are important for an increase in PEP and delayed depletion of FBP [63]. This theory claims that the PK-FFL is required for the rapid increase in PEP concentrations after glucose exhaustion. The increase in PEP assures rapid uptake of glucose upon its re-availability. Thus, high PEP concentrations are maintained after glucose exhaustion which is a supposed requirement for the resumption of glycolysis when glucose is restored [64]. However, it has also been found that that this FFL is present even in organisms that do not rely on high PEP concentrations to start-up glycolysis upon glucose addition, which casts doubt over this theory for the PK-FFLs sole functional existence.

The third theory discredits the importance of maintaining high PEP levels. Instead, it favours the idea that high FBP levels tend to be indicative of high flux, and that the PK-FFL aids in pulling at the intermediates in lower glycolysis, thereby reducing the products of glyceraldehyde 3-phosphate dehydrogenase (GAPDH). Since GAPDH functions close to equilibrium and is very sensitive to mass action, the rapid removal of its products in this scenario ensures that its activity increases with an increase in flux [14]. This is important, because if upper glycolysis outpaces lower glycolysis, a significant build-up op intermediate metabolites can occur in conjunction with reduced ATP production [65]. In essence, what this theory proposes is that the PK-FFL acts as a safety measure by accelerating the lower part of glycolysis when FBP starts building up to prevent a metabolic imbalance which could result in growth arrest [15]. One study of a patient with a erythrocyte PK mutation which resulted in the anomalous absence of feedforward activation of PK by FBP reported that the patient had glycolytic intermediate metabolite levels that were four times higher than normal [66]. The aforementioned study was in fact a modelling study of feedforward activation in human erythrocyte glycolysis and is remarkably pertinent to this project due to the overlap in aims. It was only discovered quite recently due to its relative obscurity, however it is of exceptional interest to the subject matter at hand and is discussed in greater depth in chapter 5.

Even though these varying theories are intriguing, they are purely speculative at this point and no study has definitively proven or discredited any of

these ideas. Indeed, though these propositions are usually rooted in some form of experimental observation, they are equally simply contradicted by other experiments. Certainly, it may even be possible that these theories could all prove to be true simultaneously. Whatever the case may be, one thing these theories seem to agree on is that the PK-FFL must be a significant and potent regulatory mechanism within glycolysis.

2.7   The role of Pi in the PK-FFL

The final factor considered in this thesis is the potential role Pi plays on the PK-FFL. Some studies on various bacterial isoforms of PK have unearthed a pronounced inhibitory effect of Pi on PK activity. Specifically, these studies showed higher half-saturating constants for the activator FBP in the presence of increased Pi concentrations, suggesting a regulatory relationship between the two effectors [67, 68, 6]. It has since been found that Pi inhibition of PK is a fairly conserved phenomenon in lactic acid bacteria and several other classes of organisms, in contrast to the high variability in its activating effector which may reflect metabolic differences in organisms based on their adaption to different environments, as discussed earlier in this review [69].

Even though the inhibitory effect of Pi on PK has been known for years, very few existing models or studies of central metabolism take this effect into account. A study on lactic acid bacteria revealed that during starvation conditions, phosphate is mostly incorporated into PEP, 3PG and 2PG or as unbound Pi. However, this shifts towards FBP and ATP during glycolysis. It was found that FBP accumulation is dependent on extracellular phosphate concentration, and that model fits to experimental data were remarkably improved when phosphate uptake is included in the model [38]. Indeed, it has been stressed that the concentration of free phosphate is a potentially important regulator, and should be included in glycolytic models as a free variable so that the total phosphate pool is conserved, i.e. so that the concentration of free Pi is dependent on the amount of glycolytic intermediates and ATP [14]. Making Pi a free variable rather than an input variable accounts for moiety conservation and allows the total phosphate pool to be conserved, as it is *in vivo* [63].

2.8   The Systems Biology approach

The use of a combination of computational modelling and experimental work, as done in this project, is a hallmark of the interdisciplinary systems biology approach to biochemistry, which eschews the reductionist approach that has dominated the field in the past in favour of an integrated, systems view of cellular function and metabolism. This is valuable as it allows for compu-

tational experimentation that is less resource-intensive and more robust, yet flexible, than traditional experiments performed in the lab. The construction of models allows for the realistic prediction of the behaviour of complex systems such as cellular metabolism under specific conditions and with various perturbations. The maturation of this comparatively new field in biology has seen various approaches to metabolic modelling with varying levels of success and applicability. A study by Teusink *et al* used the novel approach of attempting to use the kinetic data measured *in vitro* to attempt to describe glycolysis as it is *in vivo*, instead of fitting the data to the observed behaviour of the pathway [70]. This study was one of the first of its kind, and separated the metabolic modelling field into two distinct approaches: The more traditional "top-down" approach and the novel "bottom-up" approach. The phenomenological top-down approach goes from a general, broad view of the system as a whole and tries to break it down into its smaller operating components, whereas the mechanistic bottom-up approach starts with acquiring knowledge about the fundamental working sub-units of a system that gives rise to the more complex system. The bottom-up approach by Teusink *et al* was considered a successful feasibility study for modelling yeast glycolysis in terms of its constituent enzymes. Though not free from criticism and dispute, it lay the groundwork for various improvements, alterations and adaptations to these types of models over the years. As such, the approach in this thesis aims to build on one such a mechanistic model by Du Preez *et al* [71] that has sprouted from the original Teusink study in yet another attempt to refine its predictive power.

In terms of metabolic modelling, a bottom-up approach means that kinetic models are constructed via the description of individual reactions within a given pathway. The kinetic behaviour of each enzyme that catalyses these reactions is dictated by its unique characteristics, and this enzyme behaviour can be described mathematically by various models that have been developed to describe enzyme kinetics. This results in the derivation of a rate equation unique to each enzyme that is based on its substrates, products and effectors and how all these components interact to determine the velocity with which the reaction it catalyses proceeds. These equations are then fitted to experimental kinetic data obtained for each enzyme in isolation. The kinetic equations with its set of kinetic parameters, as well as the full pathway stoichiometry are then used to construct ordinary differential equations (ODEs), and the full set of interdependent ODEs for a given pathway can be integrated over time to simulate changes in metabolite concentrations. This allows for the visualisation of the change in concentration of the intermediary metabolites when the kinetic parameters of each step is known. As such, the model is constructed by fitting each equation individually to its own discrete biochemical data-set, which makes this approach especially rigorous [70]. After model construction comes model validation, and this essential step of kinetic modelling requires

demonstrating that the full model which has been constructed from the characterisation of enzymes in isolation can satisfactorily predict the steady state flux and metabolite concentrations of its pathway over time. As such, when the model is used as a whole it is not fitted to experimental data, but instead predicts or attempts to simulate it in an attempt to discern whether the proposed mechanisms can explain the observed behaviour of the system [72].

This project employs several of these key aspects of the system biology approach. The following chapter deals with the kinetic characterisation of the enzyme of interest which would allow the selection of a PK rate equation based on its unique kinetic behaviour in response to its known effectors. The kinetic parameters obtained in Chapter 3 are used to populate an existing glycolytic model for yeast glycolysis which we attempt to validate in Chapter 6.

Chapter 3

Kinetic characterisation of yeast pyruvate kinase

3.1   Introduction

The objectives for this chapter were to capture the kinetic effects of both FBP and Pi on PK activity. To this end we kinetically characterised yeast PK. Cell-free extracts of the X2180 strain of *S. cerevisiae* were used to perform LDH-coupled spectrophotometric assays. The X2180 strain was used as this was the strain used to develop the detailed mechanistic model we adapt in this study [71]. The activation of PK by FBP is a well-documented phenomenon, however, in order to fully describe the FFL it is necessary to have a precise description of the kinetic behaviour of yeast PK both under standard conditions and when activated by FBP. Furthermore, even though PK inhibition by Pi is alluded to in literature, there seems to be no full description of either the extent or mechanistic origins of this effect. It seems likely that Pi would affect numerous enzymes in glycolysis [38], which is certainly a confounding factor in this study. However, these assays may provide insights on how Pi affects not only PK, but also the PK-FFL.

These assays served to provide the experimental data that is necessary to estimate the kinetic parameters used in the model construction, and also allowed for comparison of different kinetic equations in order to possibly shed light on the mechanisms by which FBP and Pi exert their respective activating and inhibitory effects. As such, these assays were performed under four conditions, namely; control conditions, with FBP, with Pi and also with a combination of both FBP and Pi. In this chapter, the focus is on the experimental data and the effects of FBP and Pi on PK's binding constants and other kinetic parameters is only described semi-quantitatively. The utility of these assays in this study is two-fold: Comparative analysis of the PK kinetic parameters could provide a better understanding of how the two proposed effectors work

24

to alter PK activity. Secondly, these kinetic data were used in Chapter 4 where a full theoretical analysis is performed by fitting novel PK rate equations to the data and obtaining numerical values for the parameters, and then comparatively analysing these model fits. For model construction, it is necessary to quantify the kinetic parameters of each enzyme in the system, a feat which Teusink [70] and (to some extent) Du Preez [71] have already accomplished in the construction of their models. However, since we are adapting the dupreez6 mechanistic model specifically with regards to its description of PK activity, it is necessary to independently determine PK kinetics. This is especially important since we are including previously omitted terms for FBP activation and Pi inhibition, as the kinetic constants for these two effectors were not included in the original model. This data thus also serves to aid in parameterising the full glycolytic model which we attempt to validate in Chapter 6.

3.2   Materials and methods

3.2.1   Buffers and solutions

All buffers, solutions and media were prepared with reverse osmosis water and autoclaved unless explicitly stated otherwise. Reagents and metabolites sourced from Sigma-Aldrich and Merck & Co..

3.2.2   Culturing *S. cerevisiae* X2180 cells

A stock solution of 100 μL *S. cerevisiae* strain X2180 was used to prepare a spread plate on solid yeast growth media (YGM) (10 g/L yeast extract, 20 g/L peptone, 20 g/L glucose and 20 g/L agar) which was incubated at 30 °C overnight. A streak plate was prepared from the spread plate and a single colony of X2180 cells was used to prepare a starter culture by inoculating liquid YGM (100 mM Potassium phthalate, 1% m/v glucose and 6.7 g/L yeast nitrogen base) which was placed on an orbital shaker at 30 °C and allowed to grow overnight. The starter culture was transferred aseptically to 400 mL liquid YGM (1% v/v) and the Erlenmeyer flasks were incubated at 30 °C on an orbital shaker for the yeast to grow in suspension until glucose exhaustion ($\pm$ 17-22 h). The cells were then harvested at diauxic shift. The yeast solution was transferred to Beckmann centrifuge bottles and centrifuged (3 500 rpm, 15 min, 4 °C). The supernatant was discarded, and the pellets resuspended and washed in 40 mL phosphate buffer (100 mM KH_2PO_4, pH 6.8) in Falcon tubes and centrifuged (3 500 rpm, 15 min, 4 °C), twice. Pellets were resuspended in phosphate buffer (5 % m/v) and starved for 3 h at 30 °C to allow the cells to use any remaining energy stores and glycolytic intermediates. After starvation, cells were centrifuged (3 500 rpm, 15 min, 4 °C) and pellets were stored at -20 °C.

3.2.3   Preparation of cell-free X2180 extract

For cell lysis, pellets were weighed and resuspended in 1:1 m/v 1x PIPES buffer (50 mM PIPES, 0.1 M KCl, 5 mM $MgSO_4$). Dithiothreitol (DTT) (100 mM) and phenylmethylsulfonyl fluoride (PMSF) (100 mM) were added, followed by 1:1 m/m of acid-washed glass beads. Cells were vortexed for 2 min and placed on ice for 30 s for a total of 8 cycles, and then centrifuged (3 500 rpm, 5 min, 4 °C) to pellet the beads and cell debris. The supernatant was transferred to Eppendorf tubes and centrifuged (14 000 rpm, 20 min, 4 °C) once again to further remove any remaining cellular debris. The supernatant was aliquoted into 50 µL samples which were stored at -80 °C until use. The protein concentration of the cell-free extract was measured using Bradford's reagent [73]. Bovine Serum Albumin (BSA) was prepared and used as a protein standard over a range of 0 - 4 mg/mL. A series of yeast lysate dilutions or BSA was incubated with Bradford reagent in a 96-well plate before measuring the absorbance at 595 nm using a SPECTROstar Nano Absorbance Plate Reader.

3.2.4   LDH-coupled enzyme Assays

Pyruvate kinase activity was quantified in the forward direction (due to its irreversible nature) at 30 °C by coupling the reaction to the enzyme LDH and evaluating the change in absorbance at 340 nm due to reduction/oxidation of the secondary metabolites NAD^+ and NADH with a SPECTROstar Nano Absorbance Plate Reader. A standard PK kinetic assay protocol was followed as found in the original Teusink study [70]. Assays were performed a total of 5 times in 96-well microtiter plates at varying ADP concentrations (0, 0.1, 0.2, 0.5, 0.75, 1, 1.5, 2, 3, 4, 6, 10, 15 and 20 mM) as well as varying PEP concentrations (0, 0.1, 0.2, 0.5, 1, 1.5, 2, 3, 4, 5, 8 and 10) with 0.8 mM NADH, 1x PIPES buffer, 0.2 µL LDH and cell-free extract (CFE) to a 0.025-0.07 μg/μL final protein concentration (chosen for the optimal linear range) in the absence of both FBP and Pi, with FBP (1 mM), with Pi (50 mM) and in the presence of both FBP and Pi (1 mM and 50 mM, respectively). ADP assay reactions were initiated after 2 min of stabilisation in the spectrophotometer with 5 mM PEP and allowed to proceed for 20 min. PEP assay reactions were performed with 10 mM ADP and an additional 6 mM $MgSO_4$ to ensure sufficient cofactors and were also initiated with PEP after 2 min of stabilisation. Assays with FBP were initiated with the cell extract instead of PEP to prevent other enzymes in the lysate from consuming the FBP.

3.3   Results and discussion

The PK kinetic assays resulted in the saturation curves for ADP and PEP depicted in Fig 3.1 and Fig 3.2 both in the absence and presence of FBP and Pi. These curves provide greater insights into the mechanisms by which

FBP and Pi regulate PK activity. While it is generally known that FBP activates PK via allosteric regulation, Pi inhibition remains poorly described in literature.
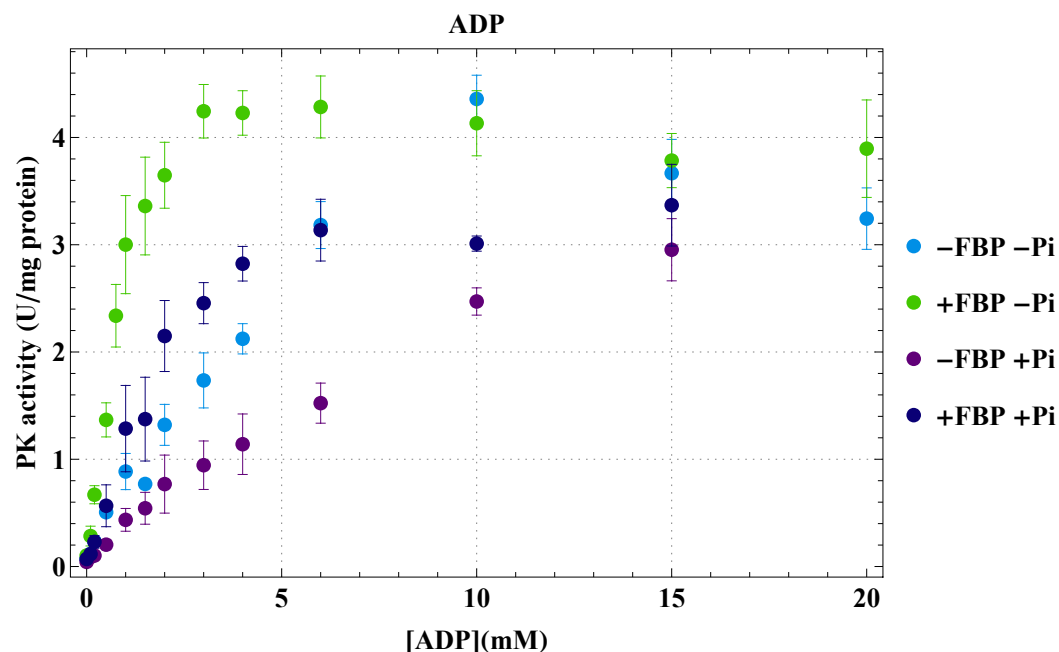
Figure 3.1: Substrate saturation curves for yeast PK substrate ADP under control conditions (-FBP -Pi, blue), with 1 mM FBP (+FBP -Pi, green), with 50 mM Pi (-FBP +Pi, purple) and with 1 mM FBP and 50 mM Pi (+FBP +Pi, navy). ADP concentrations shown on X-axis in mM. PK activity shown on the Y-axis in U/mg protein. Three independent experiments were performed (n = 3) for a total of five technical repeats. Error bars represent standard error of the mean (SEM).

The results for assays with neither activator nor inhibitor (- FBP -Pi) as shown in blue for both substrates ADP and PEP show positive cooperativity apparent from its sigmoidal shape. Even though PK displays sigmoidal kinetics towards both substrates the allosteric effect seems to be more pronounced for PEP. As displayed in green, it is evident that FBP allosterically activates PK (+ FBP -Pi), resulting in a shift to a hyperbolic shape for both substrate curves and decreasing the substrate concentrations required to reach half-maximal velocity. These values are denoted as $[PEP]_{0.5}$ and $[ADP]_{0.5}$, and they are similar to but not directly comparable to the K_m value in classic Michaelis-Menten kinetics [74]. These values and their implications are only discussed semi-quantitatively here. Although both $[PEP]_{0.5}$ and $[ADP]_{0.5}$ decrease in the presence of FBP, the effect is more pronounced for PEP in agreement with previous studies [43, 42, 75]. Notably, the V_{max} does not increase significantly in either case.
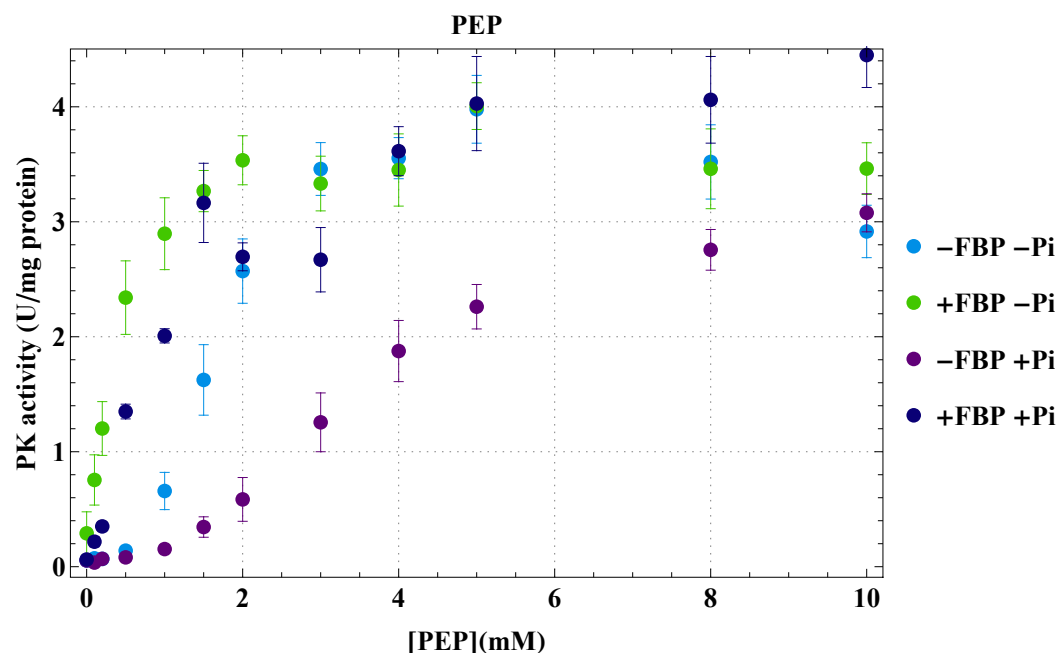
Figure 3.2: Substrate saturation curves for yeast PK substrate PEP under control conditions (-FBP -Pi, blue), with 1 mM FBP (+FBP -Pi, green), with 50 mM Pi (-FBP +Pi, purple) and with 1 mM FBP and 50 mM Pi (+FBP +Pi, navy). PEP concentrations shown on X-axis in mM. PK activity shown on the Y-axis in U/mg protein. Three independent experiments were performed (n = 3) for a total of five technical repeats. Error bars represent standard error of the mean (SEM).

In purple, the data (- FBP +Pi) show that Pi inhibits PK by increasing the half-saturating substrate concentrations, $[PEP]_{0.5}$ and $[ADP]_{0.5}$, whilst also decreasing the V_{max}. Even though it was known *a priori* that high Pi concentrations would inhibit PK, the kinetic profile could not be predicted due to a lack of understanding of the mechanism by which Pi exerts its effect. These assays elucidated that Pi acts as an uncompetitive inhibitor, which not only decreases the V_{max} slightly, but also increases $[PEP]_{0.5}$ and $[ADP]_{0.5}$, whilst retaining a slightly sigmoidal shape in the kinetic curves, once again, more notably so for PEP. The curves in navy colour depict the assays performed with both FBP and Pi (+ FBP +Pi) and indicate that FBP can overcome the inhibitory effect of Pi to an extent at the concentrations used in this experiment, as it decreases $[PEP]_{0.5}$ and $[ADP]_{0.5}$ when compared to the Pi only conditions. Even though these values are not restored to the levels seen when PK is fully activated, the activation by FBP is still evident in the new, slightly hyperbolic shapes of the saturation curves when compared to the control curves, even though they exhibit diminished activity as brought about by the Pi inhibition.

The kinetic assays show that PK exhibits sigmoidal kinetics towards both substrates under control conditions. FBP (1 mM) was found to act as an

allosteric activator whereas Pi (50 mM) acts as an uncompetitive inhibitor. A combination of both FBP and Pi shows that FBP is able to overcome the inhibitory effect of Pi to a certain extent at the concentrations used in this experiment. These assays thus served to confirm the well-described thesis that yeast PK is regulated by FBP via an FFL. Furthermore, based on these results we postulated that Pi may be able to act as an "off-switch" for the PK-FFL by suppressing FBP activation of PK. In other words, Pi may be able to selectively remove the activation of PK by FBP.

The kinetic data for PK obtained in this chapter is used in Chapter 4 to analyse rate equations for PK based on different allosteric models by evaluating their goodness-of-fit to the experimental data presented here. Thus, where the kinetic effects of PK's effectors are only described semi-quantitatively here, numerical values for these parameters will be estimated in the following chapter. The resulting parameter values from fitting the PK equation to the kinetic data is also used in Chapter 6 when we attempt to validate the full yeast glycolytic model which we have adapted to include the novel PK rate equation.

Chapter 4

Comparative analysis of novel PK rate equations

4.1   Introduction

The seminal study by Teusink *et al* [70] that attempted to discern whether yeast glycolysis can be understood in terms of the kinetic properties of its enzymes led to the development of one of the first full kinetic models for glycolysis for which the parameters were directly measured experimentally. This model has seeded the development of several other glycolytic models adapted for such factors such as cell type, cellular environment etc. As such, an existing kinetic model, dupreez6 [71] developed particularly for cell-free extracts of *S. cerevisiae* X2180 could be sourced from the JWS online database [76]. However, similar to the original study, this model does not account for the known stimulation of PK by FBP. The concentration of FBP required to maximally stimulate PK is quite low, a fact which played a major role in the decision to not account for the allosteric regulation of PK by FBP in Teusink's original study. They asserted that cellular concentrations of FBP was always significantly higher (by 1-2 orders of magnitude) than the half-saturating substrate concentration of FBP and thus PK would be perpetually saturated with FBP, and thus continually maximally stimulated. As such, they used hyperbolic Michaelis-Menten kinetics for the PK rate equation. When one considers the PK kinetics obtained in the previous chapter of this study, this does not seem like an unreasonable decision, as PK exhibits fully hyperbolic kinetics in the presence of 1 mM FBP.

Nonetheless, an older study by Hess [77] attempted to derive the PK equation with allosteric kinetics as observed experimentally. This seemed like a prudent inclusion when a study by Crow *et al* a few years later revealed that even though the intracellular concentration of FBP was much higher than the minimum concentration needed to fully activate PK, this significantly higher

FBP concentration may have been required to activate the enzyme *in vivo* to overcome Pi inhibition [6]. According to this paper, $[FBP]_{0.5}$ values obtained in kinetic studies may not be relevant *in vivo* where high concentrations of phosphate ions could be present. A study is cited where intracellular Pi concentrations were found to be 10 times higher than that of the growth media the cells were cultured in, and since 1 mM Pi increases the $[FBP]_{0.5}$ value by a factor of five, quite high FBP concentrations may be required to activate PK *in vivo*. As such, other studies since have used the allosteric equation with minor alterations [78]. Later, a paper by van den Brink *et al* claimed that the flux through PK could only be satisfactorily predicted in their study when its activating effector, FBP, was added to the Teusink model [60]. However, there seemed to be no consensus on whether including the allosteric regulation of PK improved model predictions until another paper by Kiewiet *et al* [79] was published 12 years later. Kiewiet, along with authors that were part of the original Teusink paper, aimed to revisit the *Testing Biochemistry* study and contended that they were able to improve the modelling results substantially by including the appropriate allosteric regulation where necessary, amongst other modifications. They asserted that the implementation of the allosteric regulation of PK by FBP proved crucial to these improvements, as it may play a pivotal role in cellular contexts where the FBP concentration falls below the concentration needed to maximally stimulate PK.

Considering that this project aimed to specifically study the effect of the PK-FFL on glycolysis, it seemed prudent to test PK rate equations that include a term for FBP. In order to fully describe the effect of the FFL, it may be crucial to account for the allosteric regulation of PK by FBP. Moreover, since we have postulated that Pi may act as an "off-switch" for this FFL, and considering the kinetic data in Chapter 3 that shows that Pi inhibits PK, we also decided to include Pi in the PK rate equation as an inhibitor. However, since various models for allosteric enzymes exist, it was not immediately obvious which would be the best choice. As such, a comparative analysis of three novel PK rate equations sourced and adapted from literature was performed in order to discern which would be the best choice for inclusion in the full dupreez6 model that we attempt to validate in Chapter 6. These equations are based on the classic Monod-Wyman-Changeux (MWC) [80] and Hill [81, 82] models for allosteric regulation.

The first rate equation is based on the two-substrate, two-product MWC model with concerted allosteric regulation used by Rizzi *et al* [78] and Van den Brink *et al* [60], but adapted in this study to describe inorganic phosphate as the inhibitor instead of ATP. The allosteric constant, L_o, which is the ratio between the T and R states in the absence of any ligand, was determined based on experimental pH as in Galazzo *et al* [83] and n = 3 [46, 72, 84].

$$v = \frac{V_{Max}\frac{[PEP]}{K_{PEP}}(1+\frac{[PEP]}{K_{PEP}})^{n-1}}{L_o(\frac{(1+\frac{[Pi]}{K_{Pi}})^n}{(1+\frac{[FBP]}{K_{FBP}})^n})(1+\frac{[PEP]}{K_{PEP}})^n}\frac{[ADP]}{[ADP]+K_{ADP}} \tag{4.1.1}$$

The second rate equation is based on the bi-substrate MWC equation found in Hanekom *et al* [85], once again adapted to include FBP activation and Pi inhibition

$$v = \frac{V_{Max}\frac{[ADP][PEP]}{K_{ADP}K_{PEP}}(1+\frac{[PEP]}{K_{PEP}})^{n-1}(1+\frac{[ADP]}{K_{ADP}})^{n-1}}{(1+\frac{[PEP]}{K_{PEP}})^n(1+\frac{[ADP]}{K_{ADP}})^n+L_o(\frac{(1+\frac{[Pi]}{K_{Pi}})}{(1+\frac{[FBP]}{K_{FBP}})})^n(1+\frac{[PEP]}{K_{T_{PEP}}})(1+\frac{[ADP]}{K_{T_{ADP}}})} \tag{4.1.2}$$

The third equation was based on the bi-substrate reversible Hill equation outlined by Rohwer *et al* [86], with two independent modifiers as described by Hanekom [87] and Veith *et al*, who manually calculated the K_{eq} value and mass action constant Γ for 30 ° C [69].

$$v = \frac{V_{Max}\alpha\beta\frac{1-\frac{\Gamma}{K_{Eq}}}{(\alpha+\pi)^{h-1}(\beta+\rho)^{h-1}}}{\frac{(1+\mu_1^h)(1+\mu_2^h)}{(1+\mu_1^h\sigma_1^{4h})(1+\mu_2^h\sigma_2^{4h})}+\frac{(1+\sigma_1^{2h}\mu_1^h)(1+\sigma_2^{2h}\mu_2^h)}{(1+\mu_1^h\sigma_1^{4h})(1+\mu_2^h\sigma_2^{4h})}[(\alpha+\pi)^h+(\beta+\rho)^h]+(\alpha+\pi)^h(\beta+\rho)^h} \tag{4.1.3}$$

Where $\alpha = \frac{[PEP]}{PEP_{0.5}}$, $\pi = \frac{[PYR]}{PYR_{0.5}}$, $\beta = \frac{[ADP]}{ADP_{0.5}}$, $\rho = \frac{[ATP]}{ATP_{0.5}}$, $\mu_1 = \frac{[Pi]}{Pi_{0.5}}$ and $\mu_2 = \frac{[FBP]}{FBP_{0.5}}$.

As Pi is an inhibitor and FBP an activator, $\sigma_1 < 1$ and $\sigma_2 > 1$.

4.2   Results and discussion

Data analysis and modelling was performed using the Wolfram Mathematica 12.0 software [88]. All three of the novel non-linear PK rate equations that account for Pi inhibition and FBP activation were fitted to the experimental data using the built-in *NonlinearModelFit* function using the NMinimize method, constrained only by the parameters having to be positive. The resulting fitted model curve predictions were plotted with the experimental PK kinetic data from Chapter 3 for all four assay conditions (control, with FBP, with Pi and with both FBP and Pi) for both substrates ADP (Fig 4.1) and PEP (Fig 4.2). The mean of the experimental data is represented as individual data points with error bars indicating SEM of 5 repeats (n = 3). The solid lines represent the model predictions of the PK rate equations. The resulting parameter values as estimated by the three different rate equation fits to the experimental data are shown in Table 4.1.

Parameter	MWC	Bi-MWC	Hill
K_{PEP}	0.77 ± 0.16	0.77 ± 0.20	1.41 ± 0.36
K_{ADP}	1.29 ± 0.24	0.82 ± 0.21	2.30 ± 0.31
K_{FBP}	0.23 ± 0.09	0.90 ± 0.22	2.12 ± 0.40
K_{Pi}	25.1 ± 4.70	73.7 ± 16.0	1×10^{-13}
V_{Max}	4.76 ± 0.25	5.13 ± 0.21	3.97 ± 0.19
$K_{T_{PEP}}$		2.36 ± 0.58	
$K_{T_{ADP}}$		2.99 ± 0.66	
Γ			0.03 ± 0.01
σ_1			0.68 ± 0.02
σ_2			2.03 ± 0.18
h			1.74 ± 0.15

Table 4.1: Parameter values as estimated by the three models $\pm$ standard error.

Fitting the non-linear model equations to the data resulted in reasonable trend estimations. For most of the conditions, all 3 models were able to predict the general trend of reaction rate as a function of substrate concentration, with markedly better results for PEP. However, it is worth noting the exceptions to this rule. In the second row (+FBP -Pi) of Fig 4.1. the Hill model shows a marginally better prediction of the effect of FBP on the ADP saturation curve. Both MWC models fail to accurately capture the full extent of the allosteric activation in terms of a much smaller half-saturating ADP concentration. For the PEP curve with added Pi (-FBP +Pi) in Fig 4.2, a similar shortcoming is noticeable for the Bi-MWC model which does not portray the allosteric nature of the saturation curve.

Although the Hill model advantage was already visually evident from these plots, the comparative analysis included evaluating the goodness-of-fit by the overall sum of squared deviations of calculated values from model predictions and experimental data (X^2), normalised by variance. It was determined that the Hill model described the data best as it had the lowest sum of squared differences, and this equation was thus implemented further in the full glycolytic model which we attempt to validate in Chapter 6. The selection of the Hill model was based purely on its better fit, however this does not mean that it is necessarily the better model. The Hill-type equation has more parameters than the MWC models do, and we did not add a penalty for this in our current assessment.
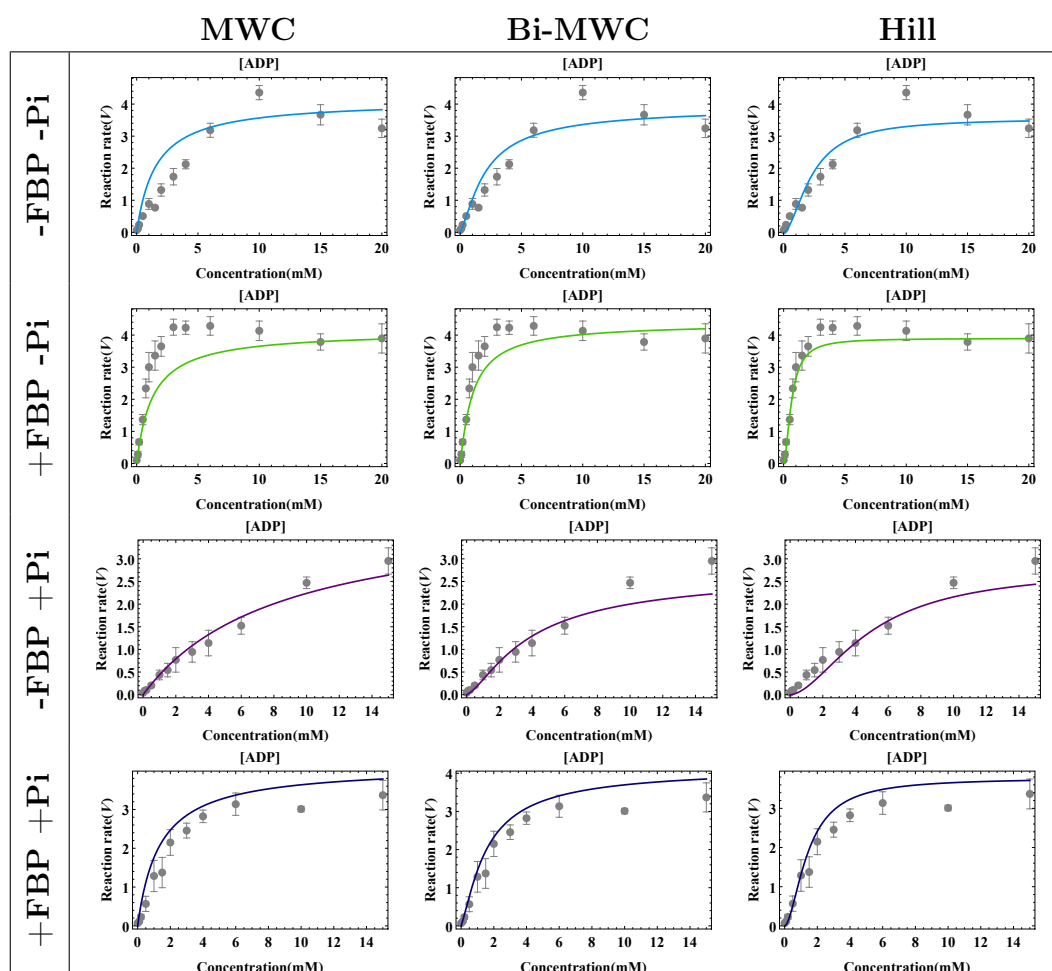
Figure 4.1: Comparison of model simulations of PK activity plotted with kinetic data for its substrate ADP at all four assay conditions: Control (-FBP -Pi), with 1 mM FBP (+FBP -Pi), with 50 mM Pi (-FBP +Pi) and with both 1 mM FBP and 50 mM Pi (+FBP +Pi). Colour lines represent model predictions. Experimental data are shown as individual data points, with error bars representing SEM 5 repeats (n = 3). Reaction rate, v, shown on the Y-axis in μmol/min/mg. Substrate concentration shown on the X-axis in mM.
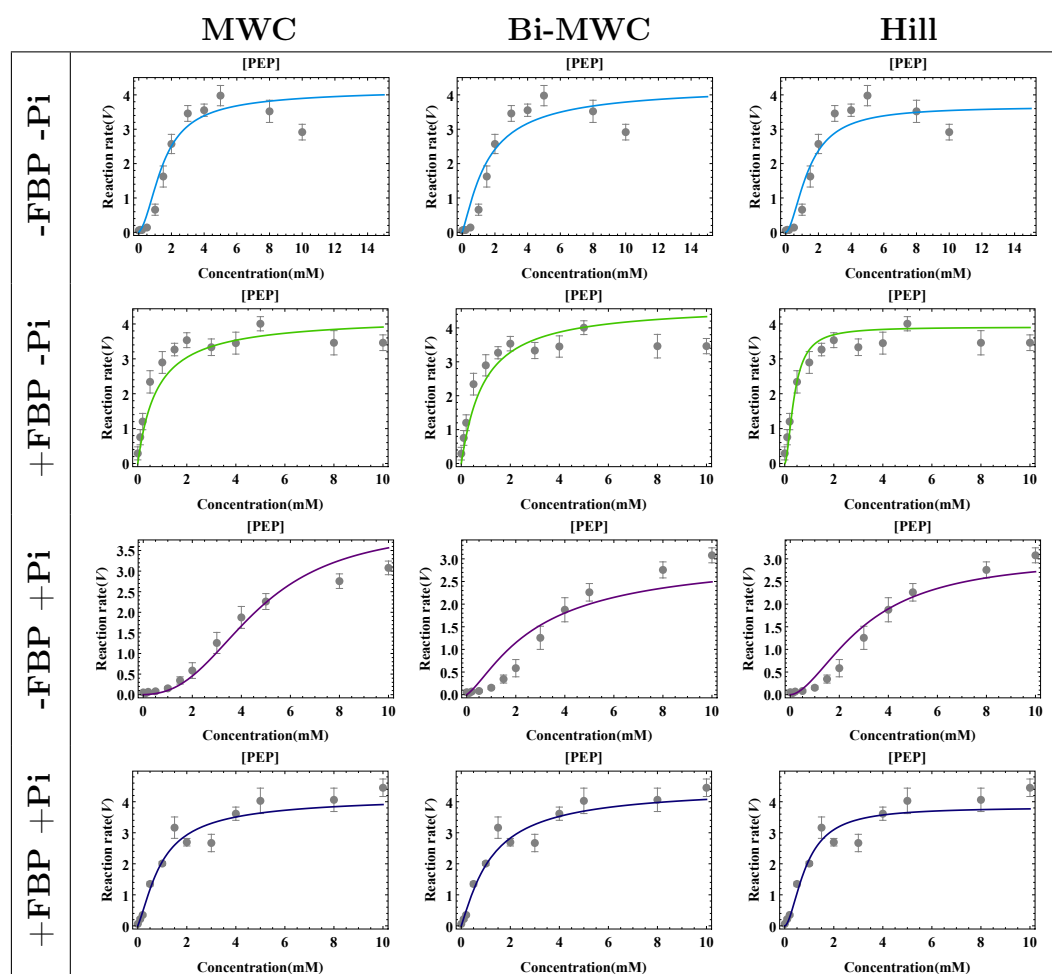
Figure 4.2: Comparison of model simulations of PK activity plotted with kinetic data for its substrate PEP at all four assay conditions: Control (-FBP -Pi), with 1 mM FBP (+FBP -Pi), with 50 mM Pi (-FBP +Pi) and with both 1 mM FBP and 50 mM Pi (+FBP +Pi). Colour lines represent model predictions. Experimental data are shown as individual data points, with error bars representing SEM of 5 repeats (n =3). Reaction rate, v, shown on the Y-axis in μmol/min/mg. Substrate concentration shown on the X-axis in mM.

Chapter 5

Core model simulations
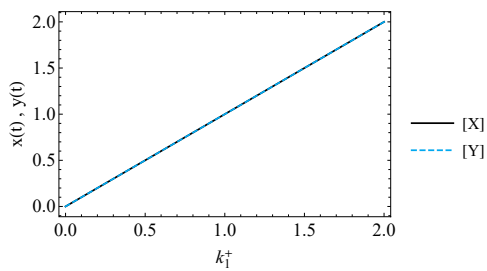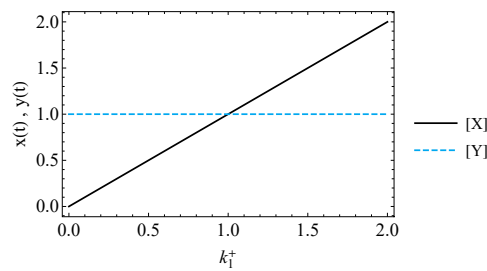
5.1   Introduction

The third objective of this project was to perform core model simulations using the Wolfram Mathematica 12.0 software [88] to try and discern whether there is some basic, generic function one can define for an FFL in the context of metabolic networks. The approach was to start with a linear metabolic pathway with mass action kinetics. The steady-state system behaviour would then be compared with and without the presence of an FFL to evaluate whether it performs a role of interest at this most basic level. The complexity of the core model system is then increased step-wise; first to evaluate the effect of having intermediate metabolites between the enzyme that produces the regulator and the regulated enzyme of the FFL. As a next step, we evaluated the effect of making these intermediate reactions form part of a highly elastic equilibrium block, as is the case with the intermediary reactions of lower glycolysis within the PK-FFL. The final increment of complexity was to make the reactions follow Michaelis-Menten kinetics instead of simple mass action kinetics to observe whether the FFL system behaviour remains consistent across all conditions. The ultimate aim of performing these simulations and analyses is to formulate a hypothesis for the potential role FFLs play within metabolic networks.

5.2   Simple FFL system
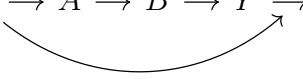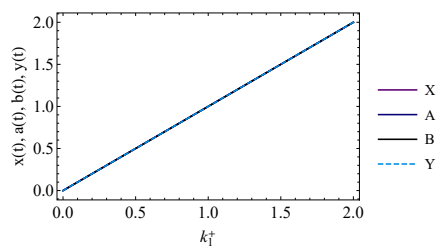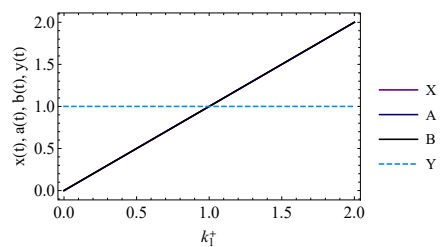
The first minimal core model, the most basic FFL system possible, was compared to a reference model with the same steady state but with no FFL. Since the FFL effect is being evaluated at the most fundamental level in this system, mass action kinetics were used as it is easy to solve for steady state solutions using these kinetic equations. This system included only two metabolites, X and Y, and the irreversible reaction linking them (v_2), along with substrate influx (v_1) and product outflow (v_3). The FFL was set up such that the first

metabolite of the pathway, X, stimulated the conversion of the second metabolite, Y, by stimulating the third enzyme of the pathway. Table 5.1 compares these two systems in terms of their reaction rates, steady state kinetic constants and the dependency of the regulated metabolite Y on the substrate influx rate. The first difference to note between these two systems is that the reaction rate v_3 is now not only dependent on the concentration of [Y], but also on the concentration of the regulating metabolite [X]. In the steady state, all metabolites are constant. As such, considering the rate of change of the metabolites X and Y as zero allows us to solve the rate equations for the steady state. Doing so reveals yet another core difference between the two systems: The introduction of the FFL makes the regulated metabolite Y independent of k_1^+, in other words, independent from substrate influx. This result is also presented graphically in the bottom panels of Table 5.1, where one can see that the metabolite being regulated becomes independent of the substrate influx rate in the FFL system. What this means in practice is that with an FFL the substrate influx rate can be increased without the accumulation of the intermediate Y.

No FFL	FFL
$\xrightarrow{V_1} X \xrightarrow{V_2} Y \xrightarrow{V_3}$	$\xrightarrow{V_1} X \xrightarrow{V_2} Y \xrightarrow{V_3}$
$v_1 \to k_1^+$ $v_2 \to k_2^+[X]$ $v_3 \to k_3^+[Y]$	$v_1 \to k_1^+$ $v_2 \to k_2^+[X]$ $v_3 \to k_3^+[Y][X]$
$x[t] \to \dfrac{k_1^+}{k_2^+}$ $y[t] \to \dfrac{k_2^+}{k_3^+}$	$x[t] \to \dfrac{k_1^+}{k_2^+}$ $y[t] \to \dfrac{k_1^+}{k_3^+}$

Table 5.1: Minimal core model: Comparison of system kinetics with and without an FFL. Parameter values for simulations: $k_1 = 1, k_2 = 1, k_3 = 1$.

5.3   Intermediates: Irreversible reactions

No FFL	FFL
$\xrightarrow{V_1} X \xrightarrow{V_2} A \xrightarrow{V_3} B \xrightarrow{V_4} Y \xrightarrow{V_5}$	$\xrightarrow{V_1} X \xrightarrow{V_2} A \xrightarrow{V_3} B \xrightarrow{V_4} Y \xrightarrow{V_5}$
$v_1 \to k_1^+$ $v_2 \to k_2^+[X]$ $v_3 \to k_3^+[A]$ $v_4 \to k_4^+[B]$ $v_5 \to k_5^+[Y]$	$v_1 \to k_1^+$ $v_2 \to k_2^+[X]$ $v_3 \to k_3^+[A]$ $v_4 \to k_4^+[B]$ $v_5 \to k_5^+[Y][X]$
$x[t] \to \dfrac{k_1^+}{k_2^+}$ $a[t] \to \dfrac{k_1^+}{k_3^+}$ $b[t] \to \dfrac{k_1^+}{k_4^+}$ $y[t] \to \dfrac{k_1^+}{k_5^+}$	$x[t] \to \dfrac{k_1^+}{k_2^+}$ $a[t] \to \dfrac{k_1^+}{k_3^+}$ $b[t] \to \dfrac{k_1^+}{k_4^+}$ $y[t] \to \dfrac{k_2^+}{k_5^+}$
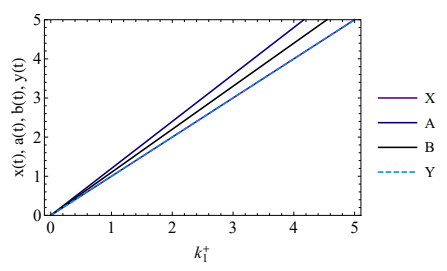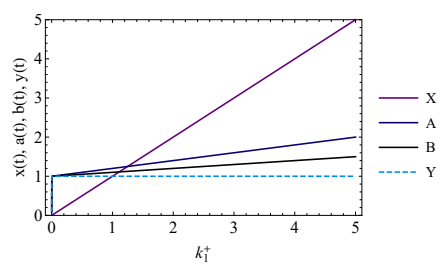
Table 5.2: Minimal core model with intermediates: Comparison of system kinetics with and without an FFL. Parameter values for simulations: $k_1 = 1, k_2 = 1, k_3 = 1, k_4 = 1, k_5 = 1$.

Setting up a slightly more complex system, the intermediate metabolites A and B were introduced between the regulating and regulated metabolite. The linear pathway now describes a system where the substrate X is first converted sequentially into the intermediate metabolite A, followed by B and then converted to the final product Y. All reactions remain irreversible in this system, and still follow simple mass action kinetics. The results depicted in Table 5.2 are largely similar to the simple FFL results of the previous section. It was found that the presence of an FFL renders only the substrate

of the regulated enzyme, Y, independent of the influx value, whereas the other intermediates A and B increase proportionally with influx. What this means in practice is that the intermediates A and B are not constant with varying influx. For a system without an FFL, an increase in k_1^+ results in all reactions speeding up to reach a new steady state at whatever the influx value is, regardless of its magnitude. Based on these results we propose that the FFL in simple systems such as these helps to keep the substrate of the regulated enzyme at a constant level as long as the regulated enzyme is sensitive to the regulator. This makes intuitive sense since the enzyme is already being activated by the loop, and as such it does not require an increase in substrate for an increase in flux.

5.4   Intermediates: Equilibrium block
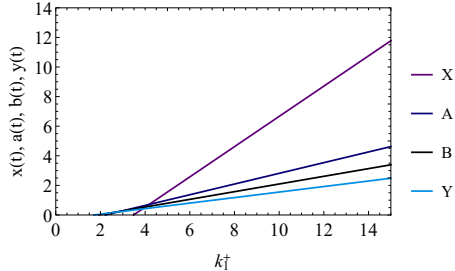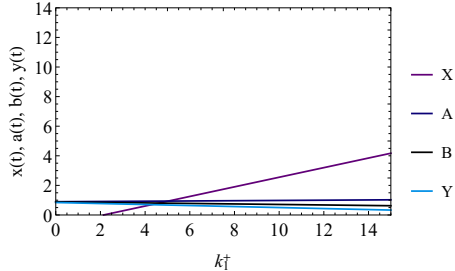
Going yet another step further in terms of complexity, the intermediate reactions were made reversible and highly elastic, forming a block of reactions close to equilibrium. This means that the reactions that fall within the loop are now quite fast and reactive, so they should be sensitive to even minor changes in intermediates to adapt their activity to the influx rate. In the bot-

No FFL	FFL
$\xrightarrow{V_1} X \overset{V_2}{\rightleftharpoons} A \overset{V_3}{\rightleftharpoons} B \overset{V_4}{\rightleftharpoons} Y \xrightarrow{V_5}$	$\xrightarrow{V_1} X \overset{V_2}{\rightleftharpoons} A \overset{V_3}{\rightleftharpoons} B \overset{V_4}{\rightleftharpoons} Y \xrightarrow{V_5}$
$v_1 \rightarrow k_1^+$ $v_2 \rightarrow k_2^+[X] - k_2^-[A]$ $v_3 \rightarrow k_3^+[A] - k_3^-[B]$ $v_4 \rightarrow k_4^+[B] - k_4^-[Y]$ $v_5 \rightarrow k_5^+[Y]$	$v_1 \rightarrow k_1^+$ $v_2 \rightarrow k_2^+[X] - k_2^-[A]$ $v_3 \rightarrow k_3^+[A] - k_3^-[B]$ $v_4 \rightarrow k_4^+[B] - k_4^-[Y]$ $v_5 \rightarrow k_5^+[Y][X]$

Table 5.3: Minimal core model with intermediates in an equilibrium block following mass action kinetics: Comparison of system kinetics with and without an FFL. Parameter values for simulations: $k_2^+ = 1, k_2^- = 0.0001, k_3^+ = 10, k_3^- = 10, k_4^+ = 10, k_4^- = 10, k_5 = 1$.

tom panel of Table 5.3 it can be seen that the FFL now results in buffering of all intermediates when glucose influx increases, in stark contrast with the no FFL system. The steady-state solution reveals that all intermediates increase linearly without an FFL, whereas the introduction of an FFL keeps all intermediates relatively steady at low concentrations relative to the substrate influx rate.

5.5   Michaelis-Menten kinetics

Table 5.4: Minimal core model with intermediates in an equilibrium block following Michaelis-Menten kinetics: Comparison of system kinetics with and without an FFL. Parameter values for simulations: $k^2_{mx} = 1, k^2_{ma} = 1, k^3_{ma} = 1, k^3_{mb} = 1, k^4_{mb} = 1, k^4_{my} = 1, k^5_{my} = 1, k^5_{mz} = 1, v^2_{mf} = 20, v^2_{mr} = 0.1, v^3_{mf} = 100, v^3_{mr} = 100, v^4_{mf} = 100, v^4_{mr} = 100, v^5_{mf} = 25, v^5_{mr} = 25, z = 1$.

Since our principal focus is understanding the fundamentals of metabolic regulation through FFLs, it is worth investigating whether the phenomena witnessed for systems with mass action kinetics holds when the reactions follow Michaelis-Menten enzyme kinetics, which are more commonly found within biochemical networks. As such, the reactions, including the one being regulated via an FFL, was given Michaelis-Menten kinetics instead of simple mass action kinetics to test if the system would still exhibit the same behaviour. In this system, V_2 was assigned a relatively low value, which is necessary to maintain a high concentration of the regulating metabolite X. Additionally, the maximal velocity of the reaction being regulated via the FFL (V_5) was made 4 times lower than the preceding reactions. This is necessary because

the enzyme being regulated must be limiting, and if this reaction rate is already high then it is not sensitive enough to the regulating metabolite X and thus the regulator will have little to no effect. Table 5.4 shows the reversible Michaelis-Menten rate equation derived for this system for v_5 with and without feedforward regulation.The graphs show how the presence of the FFL affects the concentrations of the intermediates when the influx value k_1 increases. At $k_1 = 15$, the concentrations of the intermediates in the system without feedforward regulation are five times higher than the system being regulated by an FFL. It was found that when k_1 is increased higher still, it can result in up to a tenfold difference in intermediate concentrations between the two systems. These results are congruent with our earlier findings, showing that the presence of the FFL helps with maintaining lower levels of the intermediates between the regulating and regulated metabolite. Thus, the fundamental finding holds not only for systems following mass action kinetics, but also for those following Michaelis-Menten kinetics.

5.6 Conclusions

Based on these core model simulations we formulated the preliminary hypothesis that the function of the metabolic FFL is to buffer intermediates between the regulating and the regulated metabolite when flux through the pathway increases. For a metabolic network like glycolysis, this means that it would prevent the accumulation of the intermediates of lower glycolysis after a glucose pulse to the pathway. This stabilising influence of the PK-FFL on the metabolite pools would thus be able to minimise transient fluctuations in the concentrations of the metabolites within the loop during variations in glucose availability. The synthesis of this hypothesis depended on summarising the results above for the various systems in a generic way, and we are curious to see whether this would hold for any pathway. However, most pertinent to our project specifically is a system with a linear pathway and an intermediate metabolite that positively stimulates one of the downstream reactions. These simulations highlight some important factors necessary for such a FFL system, the first of which is the need for a high concentration of the regulating metabolite X as brought about by the requirement for a low v_2, the reaction which uses X as a substrate. Notably, this is usually the case for the PK-FFL system as FBP concentrations are usually relatively high *in vivo*. Another consideration is that the enzyme must be limiting in some way, thus v_2 is also made irreversible. This once again is reflected in the PK-FFL system as the reaction catalysed by PFK producing the regulator FBP is also irreversible. Lastly, the reaction being stimulated v_5 is also made comparatively slow as otherwise the regulator X will have no effect on the rate. It is necessary that this reaction is sensitive to the concentration of its regulating metabolite. The aforementioned considerations informed our choices of parameter values during

simulations and reinforced the idea that a system that is effectively regulated via an FFL seems to possess certain generic qualities.

The proposed core model hypothesis speaks to several advantages that positive FFL regulation may confer to a pathway. As explored in Chapter 2, it has been found that decreased PK activity leads to the build-up of the intermediates of lower glycolysis, which is the first hint that the FFL that stimulates its activity may exist to prevent this from happening. There are many reasons why a cellular system would want to avoid such an accumulation of products, such as: maximising efficiency and avoiding waste; high concentrations of any intermediate potentially leading to cytotoxicity; an imbalance between upper and lower glycolysis which can lead to metabolic malfunctioning and growth arrest; or an increased availability of metabolic precursors that are diverted into anabolic processes. A modelling study [66] of human erythrocyte glycolysis that attempted to explore the possible role of the PK-FFL by examining steady-state solutions of glycolytic flux in the presence and absence of the FF activation step made similar conclusions to the one hypothesised here. They found that removal of the FFL had little to no effect on the glycolytic flux, but resulted in significantly higher concentrations of the intermediates found within the loop, i.e from FBP to PEP. This was accompanied by a decrease in those intermediates upstream of the loop, like F6P and G6P. They found that in the presence of the FFL, the concentrations of the intermediates within the loop show little to no perturbation when the flux rate through the pathway changes. As such, the FFL not only has a stabilising influence on metabolite pools, but also results in increased sensitivity to changes in glycolytic flux [66].

In Chapter 6 we attempt to extrapolate the hypothesis formulated in this chapter experimentally for glycolysis in *S. cerevisiae* by analysing the pathway intermediate dynamics in the presence and absence of the PK-FFL.

Chapter 6

Analysis of glycolytic intermediate dynamics in yeast

6.1   Introduction

In order to test the core model hypothesis formulated in Chapter 5 for a real pathway, the aim of this chapter was to observe how glycolytic intermediate dynamics in a cell free extract change in the presence and absence of the PK-FFL. According to the hypothesis formed with our core model simulations, Pi may selectively remove the activation of PK by FBP, possibly allowing for the investigation of the effects of the FFL on the dynamic behaviour of the system in response to sudden glucose addition. Thus, in an experiment where Pi is added to inhibit the FFL, you should see an increase in the intermediates of lower glycolysis when compared to control conditions where the FFL is active. High Performance Liquid Chromatography (HPLC) was used to evaluate how the concentrations of pertinent metabolites change over time after a glucose pulse to the pathway. Control experiments were set up to assess a system with a fully functional PK-FFL, and this was compared to experiments where Pi was added in order to see how the glycolytic intermediate dynamics change in yeast when the FFL is supposedly inhibited. The HPLC glycolysis method used in this study was developed by Cobus van Dyk [89], a former PhD student in the Molecular Sytems Biology Lab of Stellenbosch University. The utility of this method lies in the fact that it measures radioactive counts of carbon intermediates in tandem with UV/Vis detection of cofactors at 245 nm. This means that the intermediate metabolites as well as the cofactors of glycolysis can be quantified simultaneously from the same sample.

The HPLC data obtained here serves a secondary purpose by acting as an independent data-set with which the altered glycolytic model could be validated. As such, the fifth and final objective of this study concerns itself with how the concentration of analytes change as a function of time for compari-

son to the model predictions. As mentioned previously, the research question this thesis aims to address was investigated via a two-pronged approach: that of experimental work as well as mathematical modelling. Experimentally, we obtained PK kinetic data in Chapter 3 to aid with model construction, and in this chapter we acquired yeast glycolytic intermediate data in order to validate the altered dupreez6 model.

6.2   Materials and methods

6.2.1   Incubation preparation

Cell-free extracts of *S. cerevisiae* strain X2180 were prepared as described in Chapter 3 of this thesis, and the protein concentration was once again determined using Bradford analysis.

Materials - All metabolites, purified enzymes and media components were sourced from Sigma-Aldrich. ^{14}C- glucose (^{14}C-GLC) was obtained from American Radiolabelled Chemicals Inc.

Glucose exhaustion pre-test - In order to ascertain whether assay conditions were conducive to glycolysis as well as to determine an approximation of the time it takes for 5 mg/mL of the CFE to deplete the added glucose, small-scale glucose exhaustion tests were performed before every incubation set-up. The following starting reagents were added to an Eppendorf tube to a final volume of 100 μL: The cofactors ATP and NAD (2 mM each), 1 X PIPES buffer (50 mM PIPES, 0.1 M KCl, 5 mM $MgSO_4$) and 1 mM glucose. The reaction mix was allowed to stabilise for a few minutes at 30 °C, after which glycolysis was initiated with yeast lysate to a final concentration of 5 mg/mL. Samples taken at 2 min intervals were tested for glucose content using Humor Diagnostica Combi 4/6 medi-test strips. The timescale of glucose exhaustion also aided in determining the optimal time-points at which to sample in the full incubation experiment.

Incubation preparation - The following reagents were added to an Eppendorf tube to a final volume of 1 mL: The cofactors ATP and NAD (2 mM each) and 1 X PIPES buffer (50 mM PIPES, 0.1 M KCl, 5 mM $MgSO_4$). To this, 9.5 mM of unlabelled glucose was added, as well as 5 μL ^{14}C-GLC ($\pm$ 0.5 mM) for an approximate final glucose concentration of 10 mM. For incubation lines that aimed to measure the Pi effect, 50 or 100 mM KPi buffer (Potassium Phosphate, pH 7) was added to the reaction mix. The reaction mixture was allowed to incubate in a water bath at 30 °C for a few minutes, after which glycolysis was initiated with 5 mg/mL of the yeast CFE.

Sampling - Immediately after initiating the reaction, the first 100 μL sample

was taken and added to 10 μL 50% perchloric acid (PCA) on ice in order to quench the reaction at t = 0. Further samples were then taken at various timepoints up to 100 min as optimally determined by the glucose exhaustion pre-tests. The reaction mix was allowed to incubate with the acid on ice for 10 min, after which the PCA was neutralised to pH 7 with 56 μL ice cold 1 M K_2CO_3. The Eppendorf tubes containing the timepoint samples were then centrifuged (14 000 rpm, 20 min, 4 °C) and the supernatant was transferred to HPLC injection vials.

Cofactor standards preparation - The HPLC method used requires the preparation of cofactor standards for setting up a UV/Vis calibration curve with which to quantify adenosine and nicotinamide moiety concentrations in incubation samples. These standards were prepared using stock solutions of AMP, ADP, ATP, NAD^+ and NADH in a 1:1:1:1:1 ratio. A serial dilution was prepared using the 1 X PIPES buffer used for the yeast incubations for the following cofactor concentrations: 2 mM, 1 mM, 0.75 mM, 0.5 mM, 0.25 mM, 0.1 mM and 0 mM. These standards were subjected to the same PCA/K_2CO_3 treatment to mimic extraction conditions of the incubations, as well as the resulting dilution factor.

6.2.2 HPLC

The HPLC method used for this study is a novel ion-pairing reverse phase liquid chromatography (IP-RPLC) method with tandem UV/Vis and radio-label detection developed by Van Dyk [89].

Materials - MilliQ water was used for the preparation of all mobile phases. HPLC-grade acetonitrile (ACN) was sourced from Romil. Tetrabutylammonium bisulfate (TBA) and formic acid (FA) was obtained from Sigma-Aldrich.

HPLC instrumental set-up - Chromatographic analysis was performed on the *SpectraSYSTEM* HPLC set-up with the following instrumental components: *SpectraSYSTEM* P4000 pump, *SpectraSYSTEM* AS3000 Autosampler, *SpectraSYSTEM* UV6000LP UV-Vis detector connected in series with a *LabLogic* β-RAM model 5 radio-label detector. The column used was a reverse phase Phenomenex Luna C_{18} column (5 μm).

Mobile phases - Mobile phase A (MPA): 25 mM TBA^+ and 0.1% FA in MilliQ H_2O, filtered using 0.2 μM Millipore Supor Membrane filters and sonicated for 20 min. Mobile phase B (MPB): 97.5% ACN with 2.5% MilliQ, sonicated for 30 min. Mobile phase C (MPC): MilliQ H_2O with 0.1 % FA filtered using 0.44 μM Millipore HVLP filters and sonicated for 20 min.

HPLC glycolysis method - 5 μL of each sample/cofactor standard was injected onto the column. The run-time was 20 min per sample at a flow-rate

of 1 mL/min. The method employs the following gradient: From 0 to 4.4 min 95% MPA and 5% MPB; from 5 to 12 min 70% MPA and 30% MPB; from 13 to 20 min 95% MPA and 5% MPB. Radiolabel detection is initiated 1 min after injection of the sample and is terminated after a run-time of 13 min. Scintillation fluid was mixed with column effluent in a 3:1 ratio.

6.2.3 Data analysis

Radiolabelled glycolytic intermediates - IP-RPLC analysis of the *S. cerevisiae* time-course samples resulted in chromatographic traces for most of the carbon intermediates of glycolysis. The chemical species GLC, G6P, F6P, FBP, DHAP, 3PG, ACA and ethanol (ETOH) were quantified via the radiolabel detector. Certain glycolytic intermediates such as PYR and G3P presented no peaks at their respective elution times, but are suspected to be present in the samples at undetectable concentrations. The elution times of the chemical species of glycolysis have been determined methodically during the development of the IP-RPLC method in use. Thus, each peak at a respective timepoint could be associated with a certain intermediate through the use of the retention time values outlined in Table 6.1, which were determined experimentally by van Dyk [89].

Intermediate	Retention time (secs)
GLC	38
ETOH	76
ACA	121
G6P	157
F6P	182
DHAP	195
PEP	254
3PG	445
FBP	641

Table 6.1: Retention times of pertinent glycolytic intermediates in the yeast time-course incubations as determined by van Dyk [89]

The radiolabel detector software (*Laura*) provides the radioactive counts measured per second, and the resultant chromatographic traces were then integrated using a *Wolfram Mathematica* script that was developed in the Molecular Systems Biology (MSB) lab. An example of the integrated chromatographic traces of the radiolabelled intermediates in a yeast incubation sample (t = 25) is shown in Fig 6.1. The script fits skewed normal distribution functions to the chromatographic peaks, and integration of these functions results in values for the area under the peak. This data was normalised to the total counts of each sample, and the contribution of radiolabelled impurities was also accounted for

by implementing a baseline subtraction. In order to determine how the normalised area value corresponds to ^{14}C glycolytic intermediate concentration, HK enzymatic assays were performed on the t = 0 samples to determine the initial total GLC concentration to associate it with its respective radioactive count. This ratio was then used to calculate the intermediate concentrations of all consequent time samples.
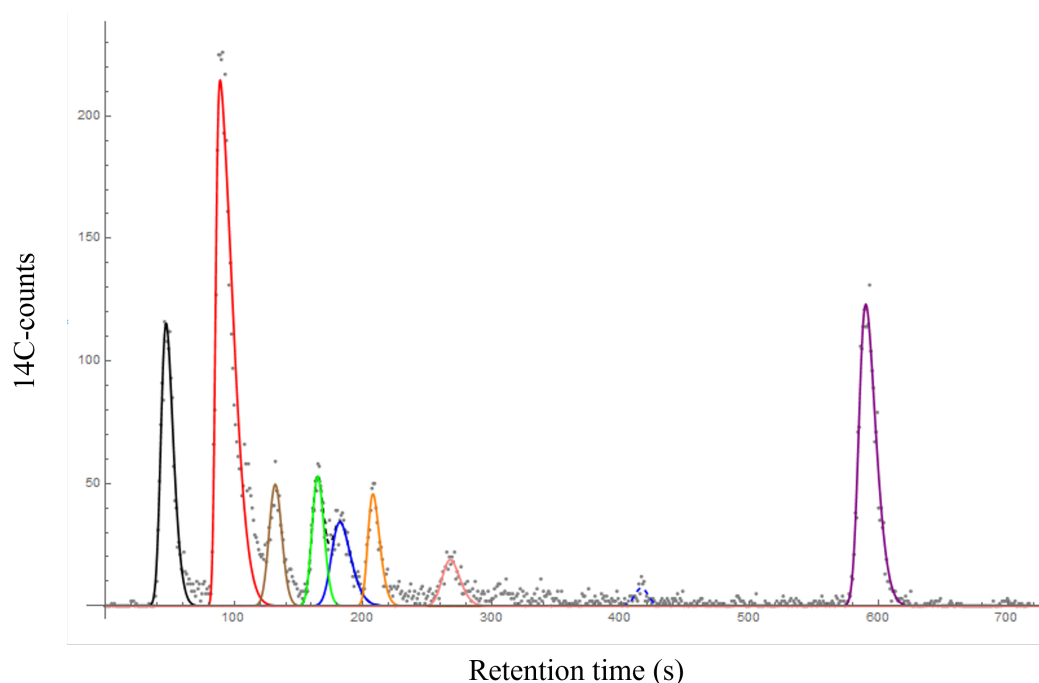
Figure 6.1: ^{14}C-chromatographic trace of a yeast time-course incubation at t = 25. The experimentally obtained radioactive traces are represented by the grey data points, and the solid colour lines are the peak fits as performed in Mathematica. Black = GLC, red = ETOH, brown = ACA, green = G6P, blue = F6P, orange = DHAP, pink = PEP, dashed blue = 3PG and purple = FBP.

Cofactors - The IP-RPLC analysis also resulted in chromatographic traces corresponding to the cofactors as detected at 254 nm via UV/Vis. Similarly to the radiolabelled intermediates, the retention times of the adenosine and nicotinamide moieties were determined experimentally by van Dyk during the development of this IP-RPLC method and are shown in Table 6.2 [89].

The UV/Vis detector results in chromatographic traces for the cofactors, and the software coupled to this detector (*Chromquest*) performs peak integration, resulting in values corresponding to the area under the peak associated with each cofactor. This data obtained from the cofactor standards were used to set up the calibration curve depicted in Fig 6.2. These curves were used to quantify the concentrations of the adenosine and nicotinamide moieties in the

Chemical species	Retention time (secs)
NAD^+	199
NADH	440-476
AMP	375
ADP	521
ATP	712

Table 6.2: Retention times of the adenosine and nicotinamide moieties separated by IP-RPLC as determined during the method development and quantified via UV/Vis detection by van Dyk [89].

yeast incubation samples using the linear relationship ($r^2 > 0.99$) between the measured area and the concentration of each cofactor.
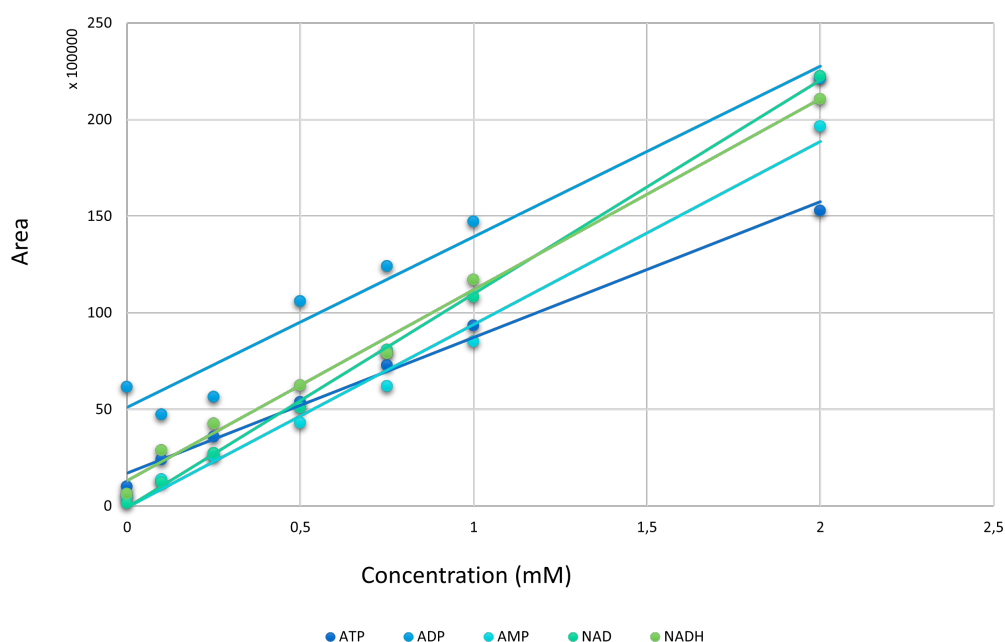
Figure 6.2: Calibration curves for the adenosine and nicotinamide moieties obtained through the preparation of cofactor standards at known concentrations. The chromatographic traces obtained via UV/Vis detection at 254 nm were integrated and the resulting area values were plotted against the concentration values of the corresponding cofactor.

6.3   Model validation

The mechanistic model used in this study was constructed by Du Preez who adapted the Teusink model for *S. cerevisiae* X2180 [71]. After the model had been constructed, it was also validated [90]. However, as we are proposing to

alter the model with a novel PK rate equation that accounts for its allosteric regulation in an attempt to better describe the FFL, it is necessary to independently validate the adapted model with our own experimental data. To this end, the novel PK equation and parameters were incorporated into the existing model to simulate how the dynamics of yeast glycolytic intermediates change over time in order to determine whether this adapted model could describe the experimental time-course data obtained via IP-RPLC.

6.3.1   Model set-up

The dupreez6 yeast glycolytic model for cell-free extracts was sourced from the JWS online database [76] and adapted by replacing the existing PK rate equation with the Hill equation (Eq 4.3.1) selected in Chapter 4 of this study. As such, the allosteric regulation of PK by FBP and Pi is now accounted for in the model. Furthermore, the rate constant for glucose addition was removed since this is a cell extract and we are interested to see what happens after a single glucose pulse to the pathway. A schema of the overall network as it is modelled in this study is shown in Fig 1.1. Barring the aforementioned changes, the dupreez6 model was used as is, with parameter values unchanged save for the incorporation of the new parameters for PK determined by the Hill model as shown in Table 4.1. Furthermore, the cofactors were considered to be conserved moieties as described in Eq 6.3.1, an assumption which is justified by the fact that the reactions regulating the nucleotide pool are much slower than the rate of glycolytic flux. Therefore, the sum of adenine nucleotides to account for the conversion of ADP to AMP and ATP (and vice versa) by adenylate kinase (AK) (Eq 6.3.1) was altered to reflect the average sum of the adenosine moeities per incubation series in the t = 0 samples as determined via IP-RPLC. Similarly, the sum of NAD^+ and NADH was adjusted to reflect the average concentration calculated per incubation series. Lastly, the protein concentration was adjusted to reflect that of the experimental conditions. This model assumes a constant Pi concentration.

$$NAD_{Total} = NAD^+ + NADH$$
$$AXP_{Total} = AMP + ADP + ATP$$
$$(6.3.1)$$

6.3.2   Model analysis

Modelling was performed in Wolfram Mathematica software and the time-course was observed by integrating the model ODEs using the NDSolve function. The dupreez6 model was extended with the parameterised PK Hill equation (Eq 4.3.1) and the initial concentrations of glucose and cofactors were adjusted in the model as quantified via IP-RPLC in the t = 0 sample.

6.4   Results and discussion

6.4.1   Yeast glycolytic intermediate dynamics

The yeast time-course incubations that were analysed in this chapter were expected to shed light on the function of the PK-FFL in glycolysis through the evaluation of how glycolytic intermediates change in the absence and presence of this FFL. The PK kinetic data obtained in Chapter 3 suggested that incubations with added Pi would have a largely inactive FFL, and the core model hypothesis predicts that this would result in glycolytic intermediates no longer being buffered. As such, Pi incubations were expected to have increased concentrations of the intermediates of lower glycolysis when compared to control incubations.

Unfortunately, both under control and Pi conditions, it was found that the concentrations of most metabolites of lower glycolysis (such as 2PG, 3PG and PEP) lie below the detection limit of the IP-RPLC method. This could mean that 50-100 mM Pi added to inhibit the PK-FFL was not a sufficient amount to significantly perturb the loop for intermediate accumulation to exceed the limit of detection and be quantifiable. Alternatively, there may yet be a difference in the concentrations of glycolytic intermediates between the control and phosphate sets of data that could prove to be significant *in vivo*, but as the concentrations are too low and cannot be quantified and compared *in vitro*, this difference remains speculative. As the two sets of data cannot be compared in this regard, the hypothesis could not be verified experimentally via that route. However, results from the initial study published by van Dyk to demonstrate the IP-RPLC method using the same yeast incubation protocol with Pi had found substantial levels of FBP accumulation after glucose exhaustion, to the extent that it was purported almost all GLC goes to FBP before lower glycolysis is able to proceed [89]. This result was substantiated by a literature survey that revealed that the accumulation of FBP was critically dependent on Pi concentration [38]. The accumulation of FBP in the presence of Pi hinted that it may be possible to observe the inhibition of the PK-FFL effect indirectly, instead of through the observation of the fluctuation of intermediates that cannot be detected.

It was postulated that the FBP build-up could be as a result of the system attempting to compensate for the inhibition by producing enough FBP to overcome it. In this way, PK can be adequately stimulated to allow lower glycolysis to proceed at a rate that prevents the accumulation of its intermediate metabolites. In order to investigate this theory, control incubations were performed and compared to Pi incubations in order to replicate the significant FBP accumulation to verify the core model hypothesis of this study.

6.4.1.1 Control incubations

The time-dependent concentrations of the glycolytic intermediates and cofactors for the *S. cerevisiae* extract control time-course incubations are shown in Fig 6.3 and 6.4, respectively. These incubations were performed and analysed in triplicate using three independent cell-free yeast extracts (n = 3) and the datapoints represent the mean of these biological repeats, with error bars indicating standard error of the mean. The mean starting concentrations these experiments were initialised with is 7.8 mM glucose, 1.3 mM ATP and 2.0 mM NAD^+. The datapoints in Fig 6.3 illustrates the concentrations of the intermediates of upper glycolysis as a function of time. GLC runs out after approximately 20 min and FBP accumulates to a maximum of around 1.5 mM at around the same time of glucose exhaustion. ETOH increases sharply soon after glucose exhaustion at 20 min, and continues to increase steadily. The intermediates of lower glycolysis remains relatively low and are not presented here. The solid and dashed lines in these figures are related to the model and will be discussed in the next section.

One unexpected and interesting outcome from these experiments was that of the cofactor dynamics. Fig 6.4 shows that ATP is rapidly depleted to almost 0 mM within the first 15 minutes after glycolysis was initiated up until the point of GLC run-out. This is coupled with an unintuitive concomitant increase in AMP within the same time-span due to the high activity of AK in yeast, which facilitates the interconversion from ADP to ATP and AMP via phosphate transfer. This swift formation of additional ATP is necessary as the effective ATP concentration required for upper glycolysis increases and this rapid depletion of ATP continues until the entire pool of adenosine has been converted into AMP. In contrast, ADP remains low and stable. In the top panel of Fig 6.4 it can be seen that NAD^+ decreases similarly between 0 and 20 min, with a resultant brief increase in NADH at the same time, before restoring to and stabilising at their respective initial values.

6.4.1.2 Phosphate incubations

The time-dependent concentrations of the glycolytic intermediates and cofactors for the *S. cerevisiae* extract time-course incubations with added Pi are shown in Fig 6.5 and 6.6. The Pi incubations were performed a total of five times (n = 5), and the datapoints represent the mean of these pooled repeats, with error bars representing the standard error of the mean. The mean starting concentrations these experiments were initialised with is 6.9 mM glucose, 1.6 mM ATP and 2.0 mM NAD^+. Three differences were noted between the control and Pi incubations. Fig 6.5 shows that the addition of Pi results in I) decreased rate of glucose consumption, as the GLC run-out time doubles from 20 to 40 min, II) decreased rate of ETOH production and III) greater build-up of FBP at the point of glucose exhaustion.
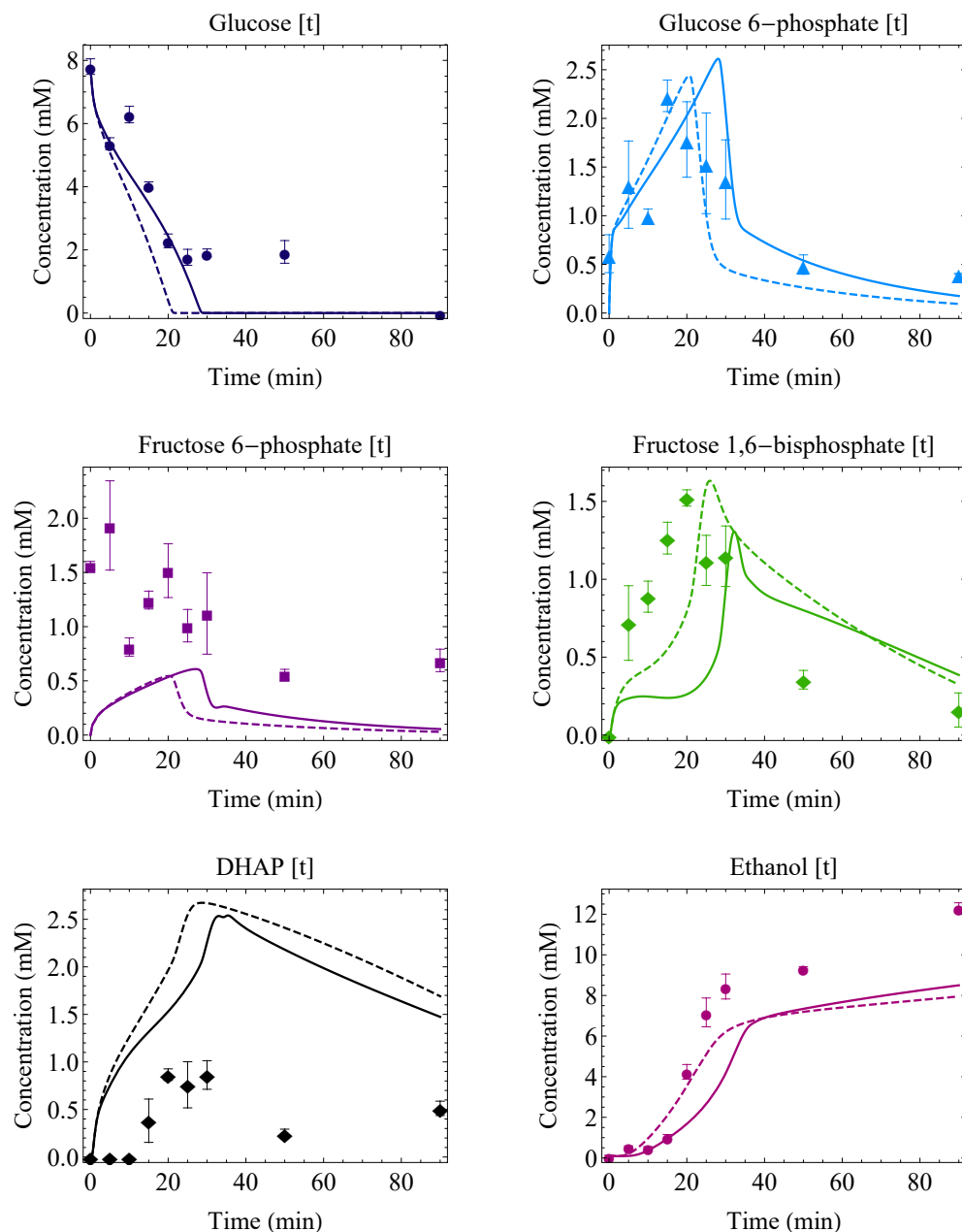
Figure 6.3: Correlation of model simulations to time-dependent concentrations of glycolytic intermediates (GLC, G6P, F6P, FBP, DHAP and ETOH) as determined via IP-RPLC analysis for control experiments. Individual datapoints represent the mean concentrations at a given time of three independent experiments ($n = 3$) and error bars show SEM. The solid lines show the altered dupreez6 model predictions. The dashed lines show the original dupreez6 model predictions.
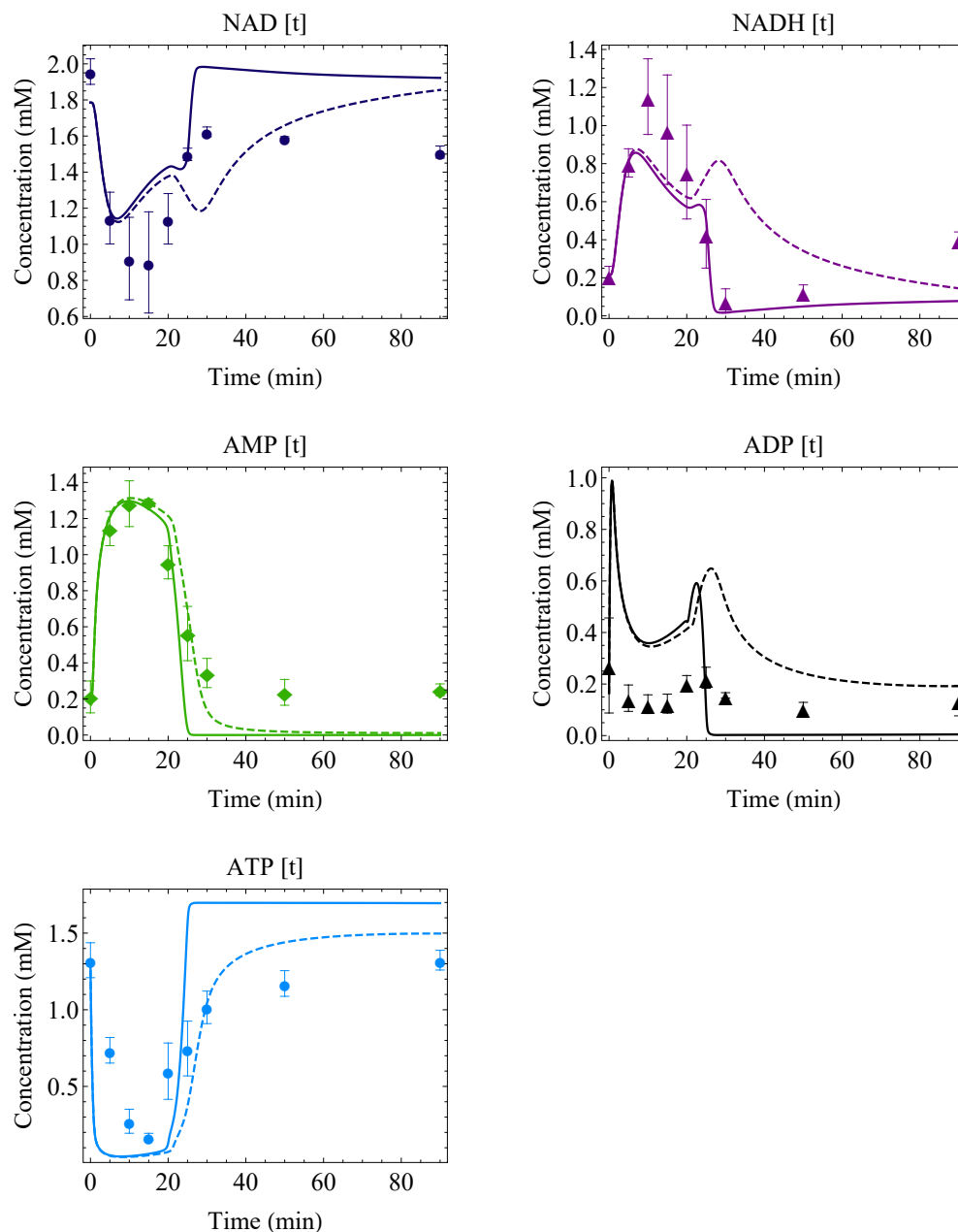
Figure 6.4: Correlation of model simulations to time-dependent concentrations of adenosine and nicotinamide moieties (NAD, NADH, AMP, ADP and ATP) as determined via IP-RPLC analysis for control experiments. Individual datapoints represent the mean concentrations at a given time of three independent experiments (n = 3) and error bars show SEM. The solid lines show the altered dupreez6 model predictions. The dashed lines show the original dupreez6 model predictions.
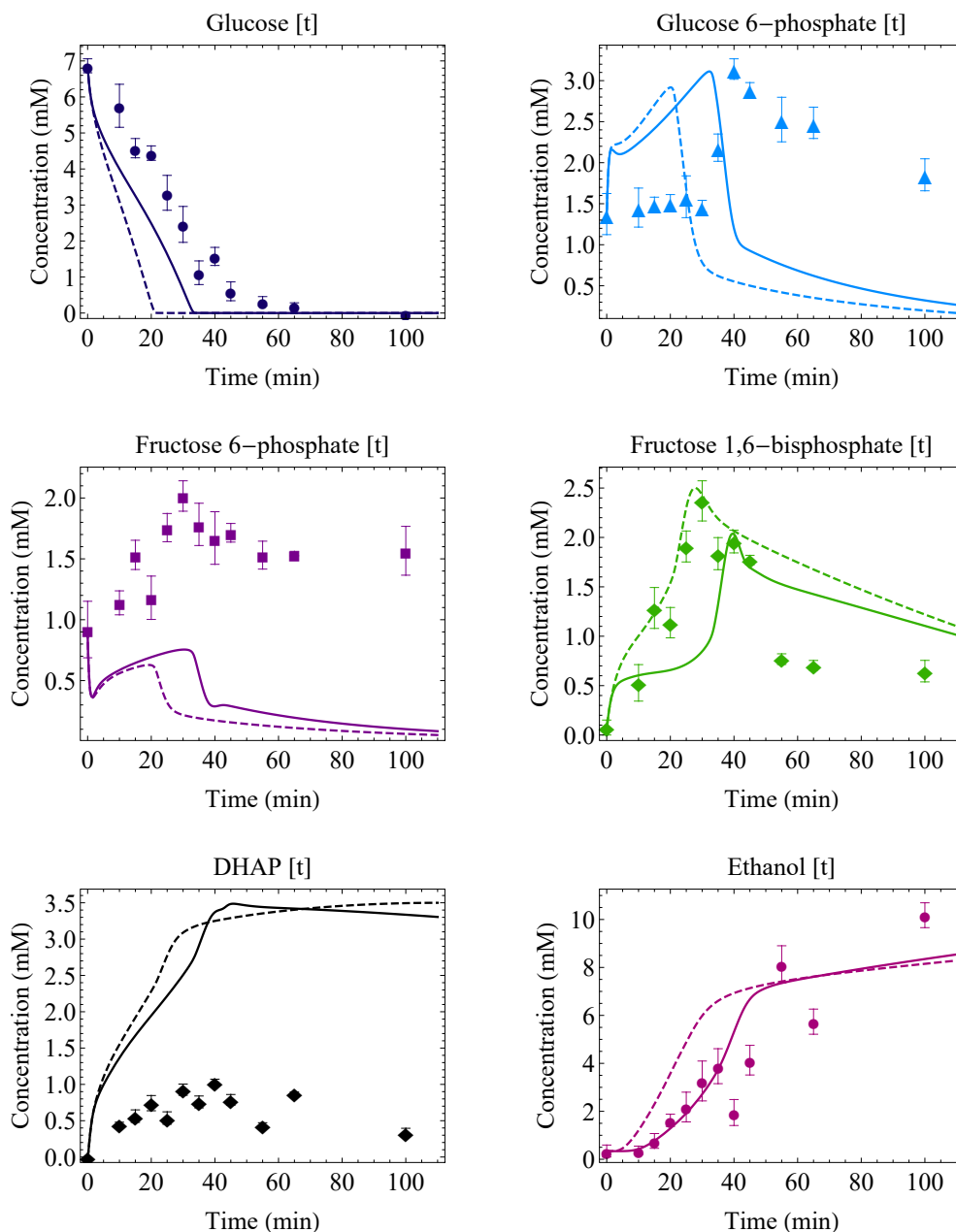
Figure 6.5: Correlation of model simulations to time-dependent concentrations of glycolytic intermediates (GLC, G6P, F6P, FBP, DHAP and ETOH) as determined via IP-RPLC analysis for phosphate experiments. Individual datapoints represent the mean concentrations at a given time of five independent experiments ($n = 5$) and error bars show SEM. The solid lines show the altered dupreez6 model predictions. The dashed lines show the original dupreez6 model predictions.
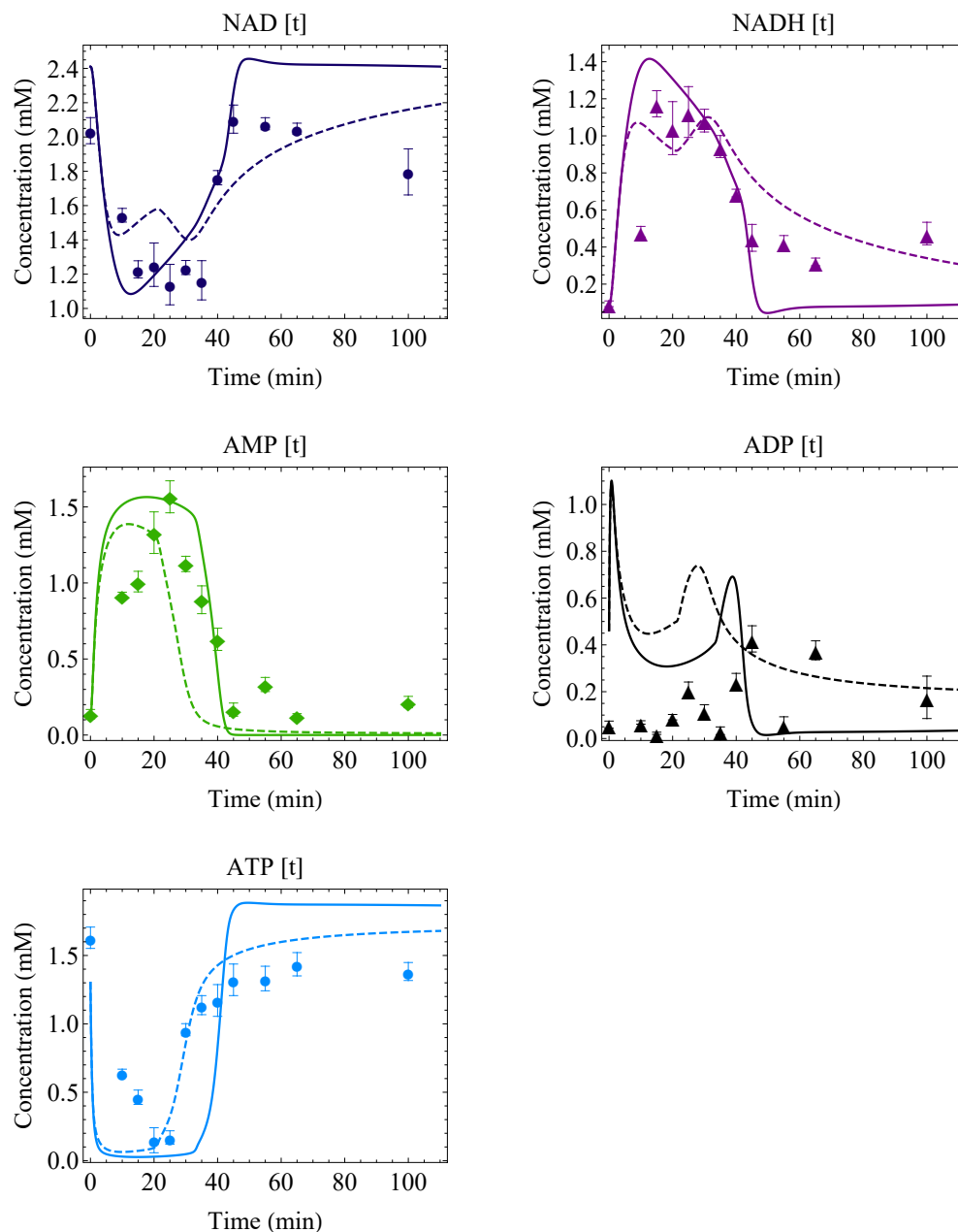
Figure 6.6: Correlation of model simulations to time-dependent concentrations of adenosine and nicotinamide moieties (NAD, NADH, AMP, ADP and ATP) as determined via IP-RPLC analysis for phosphate experiments. Individual datapoints represent the mean concentrations at a given time of five independent experiments (n = 5) and error bars show SEM. The solid lines show the altered dupreez6 model predictions. The dashed lines show the original dupreez6 model predictions.

However, even though the addition of Pi did result in increased FBP accumulation, the levels were three times lower than that reported by van Dyk. After many attempts, the substantial FBP accumulation of up to 5-6 mM reported could not be replicated in this study. Instead, FBP accumulation at the point of glucose exhaustion increased only from 1.5 mM to 2.5 mM with the addition of Pi. Subsequent enzymatic assays performed on these samples confirmed the comparatively low FBP concentrations quantified by the IP-RPLC method was not anomalous. Since this difference was of particular interest to us, a student's T-test was performed on the control and Pi datasets and the 1 mM difference at the point of peak FBP accumulation was found to be not significant.

6.4.2   Model validation

The model constructed by Du Preez resulted in a set of ODEs that describe the change for each variable metabolite in glycolysis according to the reaction velocities as catalysed by individual enzymes. These enzymes were bound by the kinetic parameters as used by Du Preez and the starting glucose and cofactor concentrations obtained via IP-RPLC. For PK, the kinetic parameters that were obtained in Chapter 4 of this study were used instead. As the dupreez6 model has been altered, it is necessary to validate it using an independent dataset that was not used in the model development. This validation is important for estimating the predictive capabilities of the model, and it requires comparison between model simulations and observed trends in data from additional experiments not used during the construction of the model. To this end, we attempted to validate the altered dupreez6 detailed kinetic model describing glycolysis in yeast cell extracts to the experimental data obtained above via IP-RPLC analysis of *S. cerevisiae* extracts. The starting concentrations of metabolites and cofactors shown in Table 6.3 as measured via IP-RPLC in the t = 0 samples were used as initial values in the model. The values in the table represent the mean of all repeats for each condition (Control and Pi). Though intermediates such as G6P and F6P were already present at quantifiable concentrations in the t = 0 sample, their initial concentrations were set to 0 mM. Similarly, the protein concentration was also set to reflect that which was analysed in the incubation samples.

Figures 6.3 and 6.4 show the concentrations of the glycolytic intermediates and cofactors over time for the control incubations as quantified via IP-RPLC, along with model predictions of both the original dupreez6 model and the adapted model. The experimental data obtained via IP-RPLC is shown as individual datapoints and represent the mean of 3 repeats, with error bars representing SEM. The solid lines represent the timecourse simulation of the dupreez6 model extended with the Hill-type PK rate equation and the parameter estimates obtained in chapter 4. The dashed lines represent the original

Metabolite	Control	Phosphate
GLC	7.802	6.862
AMP	0.211	0.137
ATP	1.323	1.301
NADH	0.215	0.090

Table 6.3: Initial concentrations of metabolites in mM as obtained via IP-RPLC analysis of time-course incubations of yeast extracts, taken at t = 0 and averaged over all repeats.

dupreez model predictions. Overall, the simulations of these two models are quite similar. The sum of the squared differences of simulated values from experimental data was calculated for both models and it was found that the adapted model was a slightly better fit. However, it is worth noting that the origanal dupreez6 model estimates a higher FBP concentration, which is also more congruent with the experimental data for this metabolite. It also predicts a slightly higher glycolytic flux as is evident from the simulation of more rapid depletion of glucose and ethanol production than what was experimentally observed. For these two metabolites the predictions of the adapted model are closer to the experimentally observed values. While it is necessary to include the simulations of the original model for comparison to the adapted model, the rest of the discussion will focus solely on the results of the adapted model.

For most metabolites, the correlation between model predictions of fluxes and time-dependent data obtained via IP-RPLC is quite good, with the exception of F6P and DHAP. It is worth reiterating that these are not model fits, but rather model predictions, and as such overall trends showing similar shapes to the data can also be considered a moderately positive outcome, even if it falls short in terms of quantifying the magnitude. Here the model accurately predicts the rate of glucose consumption, following the dynamic trace of GLC closely. Similarly, there is a good correlation between the predicted trace for G6P and the general trend of G6P concentrations obtained experimentally. However, the model underestimates the concentrations of F6P, which may be linked to its chromatographic peak overlapping with that of G6P. Deconvolution of these peaks is tricky and more likely to be error-prone, which may lead to inaccurate calculations of concentration during analysis of the IP-RPLC data. Notably, for the control dataset, the model simulates a comparable maximal FBP concentration to that quantified experimentally, but there is a delay as FBP peaks 10 minutes later in the simulation. The model also overestimates the concentrations of DHAP by approximately 1.5 mM, probably due to a slight overstatement of GAPDH activity. The rate of ETOH production is simulated fairly well, albeit with a slight underestimation. Barring the few exceptions, the altered model fares remarkably well at predicting the trends in

the intermediate metabolite timecourse data obtained for the control incubations, especially when one considers how few changes had to be implemented. Simulations of the conserved adenosine and nicotinamide moieties shown in Fig 6.4 seem exceptionally accurate, with model predictions closely following the traces obtained experimentally for all cofactors, AMP, ADP, ATP, NAD^+ and NADH.

Figure 6.5 and 6.6 shows the concentrations of the glycolytic intermediates and cofactors over time for the Pi-spiked incubations as quantified via IP-RPLC, along with model predictions. The experimental data obtained via IP-RPLC is shown as individual datapoints and represent the mean of 5 repeats, with error bars representing SEM. The solid lines represent the adapted dupreez6 model simulations, and the dashed lines show the original dupreez6 predictions. The models were adjusted with an increased Pi concentration (10 X) to see whether it could predict the concomitant changes in yeast glycolytic intermediate dynamics when the inhibitor is added. Once again the two simulations are quite similar, with a slightly better fit for the adapted model as determined by calculation of the sum of squared differences.

Similar to the control experiment, the adapted model fares reasonably well at predicting the time-dependent concentrations of most of the pertinent metabolites, but falls short with some. The model favourably predicts the slightly longer glucose exhaustion time with Pi inhibition. However, under Pi conditions the simulations of the G6P trend fares slightly worse than that of the control as the magnitude of G6P accumulation is accurate, but the peak trace is slightly premature. The simulation of the F6P trace is poor, similar to control results. However, there is a notable improvement in the trend of FBP build-up: the model accurately simulates a slight increase in FBP accumulation congruent with experimental results, and the peak timing is also notably better. Once again, DHAP is significantly overestimated. For the Pi model, the simulated rate of ETOH production once again agrees favourably with the experimental trace, and the peak concentrations are also closer in this case. Similarly accurate simulations of the cofactor traces were obtained as shown in Fig 6.6, with the data showing more or less the same trends as the control data, with the notable difference being that the model is able to simulate the slight (approximately 10 minute) delay in peaks that can be seen due to the Pi inhibition.

6.5 Conclusions

In terms of the first objective of this chapter, which was analysing the differences in glycolytic intermediate dynamics, the incapability of quantifying the intermediates of lower glycolysis made us turn our sights to FBP accumulation

to study the FFL effect. However, the FBP accumulation with added Pi was found to be not significant in these experiments. As such, the investigation of the Pi effect on the PK-FFL was inconclusive in this study. This does not necessarily negate the core model hypothesis formulated in Chapter 5, but rather that we could not test it stringently enough. These inconclusive results could also be a symptom of an incorrect assumption of how, and to what extent, Pi affects the PK-FFL. Initially, we postulated it can act as an "off-switch" for the FFL based on our observations that it inhibits PK activity, even in the presence of its feedforward activator, FBP. However, it is likely that Pi does not act exclusively on PK considering phosphate's central role in other glycolytic reactions. Furthermore, as mentioned earlier, the use of 50 - 100 mM Pi as in this study might simply not perturb the FFL strongly enough to stimulate significant FBP accumulation. As such, with Pi ruled out as a PK-FFL suppressor, there remains no way as yet of experimentally altering the magnitude of PK activation alone in order to observe the effects of its removal [66].

The second objective of this chapter was the validation of the altered dupreez6 model. With the inclusion of a novel, detailed rate equation for PK that includes its allosteric regulation by FBP and inhibition by Pi, the model for yeast glycolysis follows the IP-RPLC data closely for the majority of glycolytic intermediates in both the control and Pi experiments. As such, we can state that the model's predictive power is relatively good.

Chapter 7

Conclusion and future work

There is a need to understand the fundamental aspects of metabolic regulation. This can lead to a greater understanding of core pathways in central metabolism such as glycolysis, the dysregulation of which often leads to different disease states. Positive feedforward loops form part of one such aspect of metabolic regulation that has not yet been fully characterised in the way their counterpart, negative feedback loops, have. The aim of this project was to see whether the function of a positive feedforward loop could be described in generic terms. To investigate this question, we studied the PK-FFL in glycolysis using a systems biology approach by performing experiments with *S. cerevisiae* cells and using computational biology to perform core model simulations. Furthermore, we attempted to improve upon the mathematical description of PK's activity and flux through the pathway as a whole based on its positive feedforward regulation in a detailed kinetic model of yeast glycolysis.

To achieve this aim, five objectives were set: Firstly, the kinetic characterisation of yeast PK to capture the effects of its effectors on the enzyme's kinetic parameters. The second objective was to use this kinetic data to comparatively analyse the suitability of three different rate equations for PK derived from allosteric models which include terms for the observed regulatory effects of FBP and Pi on PK. The third objective was to perform minimal core model simulations to compare the kinetic behaviour of systems with and without positive feedforward regulation in order to formulate a preliminary core model hypothesis. The fourth aim was to attempt to illustrate this hypothesis for a real metabolic system by studying glycolysis in yeast and the role that the PK-FFL plays. The fifth objective was to validate the glycolytic model altered with the novel PK rate equation we selected with an independent set of time-course data for glycolytic intermediates.

The first objective was addressed and met in chapter 3 of this thesis. Cell-free extracts of the X2180 strain of *S. cerevisiae* were used to perform LDH-

coupled spectrophotometric assays to characterise its PK. The effect of the proposed effectors on PK's kinetic behaviour was quantified by determining its kinetic parameters under standard conditions, with FBP, with Pi and with a combination of both FBP and Pi. Analysis of the ADP and PEP substrate saturation curves obtained in these experiments established that yeast PK is allosterically stimulated by FBP via an FFL, that Pi acts as an uncompetitive inhibitor of PK, and that FBP can partially overcome this inhibitory effect of Pi at the concentrations used in this study. From these results we postulated that Pi can act as an "off-switch" for the PK-FFL, allowing us to potentially study the behaviour of glycolytic intermediates with and without such a positive feedforward loop. Chapter 4 provided the necessary parameters that were used to adapt the full, detailed kinetic model for yeast glycolysis in an attempt to improve upon its description of PK activity and flux through the pathway as a whole. Since the dupreez6 model was altered specifically with regards to its description of PK activity, it necessitated the independent determination of PK activity. Since the model was extended with previously omitted terms for FBP activation and Pi inhibition the kinetic constants for these two effectors are not present in the existing model. Thus, the second objective met in chapter 4 utilised the PK kinetic data obtained in chapter 3 to comparatively analyse the suitability of three different rate equations for PK based on the MWC and Hill models for enzymes that are allosterically regulated. This was necessary because the PK rate equation in most detailed kinetic models for glycolysis, including the dupreez6 model used in this study, does not include terms for PK regulation by FBP and Pi. Since our study is concerned with the PK-FFL which depends upon PK's activation by FBP, and our suspicion that Pi may switch off this FFL, it is imperative that the model takes these effects into account. The model predictions of these rate equations populated with the PK kinetic parameters was compared to the experimental kinetic data and it was found that even though all three models perform comparatively well at estimating PK kinetics, only the Hill model accurately predicts the hyperbolic response due to the allosteric activation of PK by FBP seen in the substrate saturation curves. Statistical analysis of these model fits confirmed the Hill model performed best, and thus the Hill equation for PK with two independent modifiers was selected to extend the full glycolytic model.

The third objective was met in chapter 5 where we performed several core model simulations with increasing complexity to evaluate whether a general trend could be observed that could be indicative of the function of FFLs within metabolic networks. It was found that both in systems where the reactions follow mass action kinetics and Michaelis-Menten kinetics, the presence of a positive FFL tends to result in substantially lower and/or more stable concentrations of the intermediates found within the loop when the influx value is perturbed. As such, the outcome of this objective was the formulation of a core model hypothesis which proposed that the function of the FFL in

metabolism is to buffer the intermediates between the regulating and the regulated metabolite when flux through the pathway increases. For a metabolic network like glycolysis, this means that it would prevent the accumulation of the intermediates of lower glycolysis found between FBP synthesis and PEP conversion to pyruvate after a glucose pulse to the pathway.

In chapter 6 we used IP-RPLC to analyse the intermediates and cofactors of glycolysis over time after a glucose pulse to the pathway. For our fourth objective, we attempted to test the core model hypothesis we formulated on a real system, and for this we tried to analyse the differences in glycolytic intermediate dynamics in the presence and absence of the PK-FFL. However, the FBP accumulation with added Pi to suppress the FFL was found to be not significant in these experiments. As such, the investigation of the Pi effect on the PK-FFL and whether it could sufficiently suppress the loop to result in a discernible difference in system behaviour was inconclusive in this study. This does not necessarily negate the core model hypothesis, as many confounding factors could be at play, most probably an incorrect assumption of how, and to what extent, Pi affects the PK-FFL. It is likely that Pi does not act exclusively on PK. Furthermore, and perhaps most importantly, Pi might simply not perturb the FFL strongly enough to stimulate significant FBP accumulation. However, based on the hypothesised and observed impeding factors, Pi can be ruled out as an effective suppressor of PK exclusively. Alternatively, there may yet have been significant differences in the dynamics of the intermediates of lower glycolysis as brought about by the successful suppression of the FFL, but we were unable to quantify these intermediates using the IP-RPLC method. However, with this analysis we did observe some unforeseen and very interesting results in terms of cofactor dynamics. The fact that ADP remains low and does not rise after initialising glycolysis with a high concentration of glucose ran counter to our intuitions. Model simulations then accurately predicted this same trend for the adenosine moieties dynamics, where AMP instead of ADP rises significantly. Clearly this result is indicative of very high adenylate kinase activity in yeast. The fifth objective of this study also addressed in chapter 6 was the validation of the altered dupreez6 model. With the inclusion of a novel, detailed rate equation for PK that includes its allosteric activation by FBP and inhibition by Pi, the adapted detailed kinetic model for yeast glycolysis follows the IP-RPLC data fairly close for the majority of glycolytic intermediates and very close for cofactors in both the control and Pi experiments.

In conclusion, based on the literature and the outcomes of the objectives pursued in this study, we propose that the generic function of the positive feedforward loop in metabolism is to buffer intermediates within the loop when flux through the pathway increases. Furthermore, we have altered and successfully validated a detailed kinetic model for yeast to account for PK stimulation by

FBP via an FFL and the inhibitory effect of Pi. Future studies that attempt to study the PK-FFL effect on glycolysis should not bargain on Pi acting effectively and exclusively to switch off the PK-FFL. To our knowledge, there remains currently no direct method of experimentally modifying PK to remove just the activation by FBP without affecting other aspects of the enzyme's kinetics. Instead, the difference in system behaviour as brought about by the presence of a positive FFL might be better studied using cells lines with PK isoforms where the PK-FFL is naturally absent, a few of which have been discussed in chapter 2 of this thesis. Furthermore, it would also be of interest to investigate whether the properties that have been observed for the PK-FFL and the suggested core model hypothesis holds for other known FFLs, for example that of LDH in lactic acid bacteria.

References

[1] Otto Warburg, Franz Wind, and Erwin Negelein. "The metabolism of tumours in the body". In: *Journal of General Physiology* 8.6 (1927), pp. 519–530.

[2] Johan H. van Heerden, Frank J. Bruggeman, and Bas Teusink. "Multi-tasking of biosynthetic and energetic functions of glycolysis explained by supply and demand logic". In: *BioEssays* 37.1 (2015), pp. 34–45.

[3] Nicolaas A. Buijs, Verena Siewers, and Jens Nielsen. *Advanced biofuel production by the yeast saccharomyces cerevisiae*. 2013.

[4] Matthew G.Vander Heiden, Lewis C. Cantley, and Craig B. Thompson. *Understanding the warburg effect: The metabolic requirements of cell proliferation*. 2009.

[5] Patrick Schrauwen, Silvie Timmers, and Matthijs K.C. Hesselink. *Blocking the entrance to open the gate*. 2013.

[6] Vaughan L. Crow and Graham G. Pritchard. "Purification and properties of pyruvate kinase from Streptococcus lactis". In: *BBA - Enzymology* 438.1 (1976), pp. 90–101.

[7] J Berg, J Tymoczko, and L Stryer. *Biochemistry, 5th edition*. 2002, Section 16.1.

[8] John W. Pelley. *Elsevier's integrated biochemistry*. 2006, pp. 47–53.

[9] N.V. Bhagavan et al. "Carbohydrate Metabolism I: Glycolysis and the Tricarboxylic Acid Cycle". In: *Essentials of Medical Biochemistry* (2015), pp. 165–185.

[10] Gerald Litwack. "Glycolysis and Gluconeogenesis". In: *Human Biochemistry*. 2018, pp. 183–198.

[11] Lukas Bahati Tanner et al. "Four Key Steps Control Glycolytic Flux in Mammalian Cells". In: *Cell Systems* 7.1 (2018), 49–62.e8.

[12] Jason W. Locasale. "New concepts in feedback regulation of glucose metabolism". In: *Current Opinion in Systems Biology* 8 (2018), pp. 32–38.

[13] Herbert M Sauro. "Control and regulation of pathways via negative feed-back". In: (2017).

[14] Bas Teusink, Herwig Bachmann, and Douwe Molenaar. "Systems biology of lactic acid bacteria : a critical review". In: *Microbial Cell Factories* 10.Suppl 1 (2011), S11.

[15] Johan H. Van Heerden et al. "Lost in transition: Start-up of glycolysis yields subpopulations of nongrowing cells". In: *Science* 343.6174 (2014).

[16] Rei Noguchi et al. "The selective control of glycolysis, gluconeogenesis and glycogenesis by temporal insulin patterns". In: *Molecular Systems Biology* 9.1 (2013), pp. 1–12.

[17] Rui Curi et al. "Regulatory principles in metabolism -Then and now". In: *Biochemical Journal* 473.13 (2016), pp. 1845–1857.

[18] Bernard Crabtree and Eric A. Newsholme. "Sensitivity of a Near-Equilibrium Reaction in a Metabolic Pathway to Changes in Substrate Concentration". In: *European Journal of Biochemistry* 89.1 (1978), pp. 19–22. eprint: `https : / / febs . onlinelibrary . wiley . com / doi / pdf / 10 . 1111/j.1432-1033.1978.tb20891.x`.

[19] Eric A. Newsholme and Bernard Crabtree. "Theoretical principles in the approaches to control of metabolic pathways and their application to glycolysis in muscle". In: *Journal of Molecular Cell Cardiology* 11.9 (1979), pp. 839–56.

[20] Jan Hendrik S. Hofmeyr and Athel Cornish-Bowden. *Regulating the cellular economy of supply and demand.* 2000.

[21] Christian M Metallo and Matthew G Van der Heiden. "Understanding metabolic regulation and its influence on cell physiology". In: *Molecular Cell* 49.3 (2016), pp. 388–398.

[22] H. Kacser, J. A. Burns, and D. A. Fell. "The control of flux". In: *Biochemical Society Transactions* 23.2 (1995), pp. 341–366.

[23] Reinhart Heinrich and Tom A. Rapoport. "A Linear Steady-State Treatment of Enzymatic Chains: General Properties, Control and Effector Strength". In: *European Journal of Biochemistry* (1974).

[24] David Fell. *Understanding the Control of Metabolism.* Jan. 1997.

[25] B. Crabtree and E.A. Newsholme. "A Quantitative Approach to Metabolic Control". In: ed. by Bernard L. Horecker and Earl R. Stadtman. Vol. 25. Current Topics in Cellular Regulation. Academic Press, 1985, pp. 21–76.

[26] B. Crabtree and E. A. Newsholme. "The derivation and interpretation of control coefficients." In: *The Biochemical journal* (1987).

[27] Michael A. Savageau. "Biochemical systems analysis: I. Some mathematical properties of the rate law for the component enzymatic reactions". In: *Journal of Theoretical Biology* 25.3 (1969), pp. 365–369.

[28]   Albert K. Groen and Hans V. Westerhoff. "Modern Control Theories: a Consumers' Test". In: *Control of Metabolic Processes*. Ed. by Athel Cornish-Bowden and María Luz Cárdenas. Boston, MA: Springer US, 1990, pp. 101–118.

[29]   Thomas E. Gorochowski, Claire S. Grierson, and Mario di Bernardo. "Organisation of feed-forward loop motifs reveals architectural principles in natural and engineered networks". In: *bioRxiv* (2017).

[30]   Lee J. Sweetlove and Alisdair R. Fernie. "Regulation of metabolic networks: Understanding metabolic complexity in the systems biology era". In: *New Phytologist* 168.1 (2005), pp. 9–24.

[31]   Uri Alon. *An Introduction to Systems Biology*. 2007.

[32]   Lewi Stone, Daniel Simberloff, and Yael Artzy-Randrup. "Network motifs and their origins". In: *PLOS Computational Biology* 15.4 (2019), e1006749.

[33]   Emma Watson, L Safak Yilmaz, and Albertha J M Walhout. "Understanding Metabolic Regulation at a Systems Level : Metabolite Sensing , Mathematical Predictions , and Model Organisms". In: *Annual Review of Genetics* 49 (2015), pp. 553–578.

[34]   Mathieu Cloutier and Edwin Wang. "Dynamic modeling and analysis of cancer cellular network motifs". In: *Integrative Biology* 3.7 (2011), pp. 724–732.

[35]   Durreshahwar Muhammad et al. *More than meets the eye: Emergent properties of transcription factors networks in Arabidopsis*. 2017.

[36]   Onn Brandman and Tobias Meyer. "Feedback Loops Shape Cellular Signals in Space and Time". In: *Science* 322.October (2008), pp. 390–396.

[37]   Madalena Chaves et al. "Dynamics of complex feedback architectures in metabolic pathways". In: *Automatica* 99 (2019), pp. 323–332.

[38]   Jennifer Levering et al. "Role of phosphate in the central metabolism of two lactic acid bacteria - A comparative systems biology approach". In: *FEBS Journal* 279.7 (2012), pp. 1274–1290.

[39]   Shinya Fushinobu et al. "Allosteric activation of L-lactate dehydrogenase analyzed by hybrid enzymes with effector-sensitive and -insensitive subunits". In: *Journal of Biological Chemistry* 271.41 (1996), pp. 25611–25616.

[40]   Marnette Coetzee. "Feedforward activation in metabolic systems". In: March (2016).

[41]   Giovanna Valentini et al. "The allosteric regulation of pyruvate kinase: A site-directed mutagenesis study". In: *Journal of Biological Chemistry* 275.24 (2000), pp. 18145–18152.

[42] J. R Hunsley and C. H Suelter. "Yeast Pyruvate Kinase". In: *The Journal of Biological Chemistry* 244.18 (1969), pp. 4819–4822.

[43] Eckhard Boles et al. "Characterization of a Glucose-Repressed Pyruvate Kinase (Pyk2p) in Saccharomyces cerevisiae That Is Catalytically Insensitive to Fructose-1 , 6-Bisphosphate". In: *Journal of Bacteriology* 179.9 (1997), pp. 2987–2993.

[44] Ulrike Johnsen et al. "New views on an old enzyme: allosteric regulation and evolution of archaeal pyruvate kinases". In: *FEBS Journal* 286.13 (2019), pp. 2471–2489.

[45] Enrique Rozengurt, Luis Jimenez de Asua, and Hector Carminatti. "Some kinetic properties of liver pyruvate kinase (Type L)". In: *The Journal of Biological Chemistry* 244.12 (1969), pp. 3142–3148.

[46] Melissa S. Jurica et al. "The allosteric regulation of pyruvate kinase by fructose-1,6-bisphosphate". In: *Structure* 6.2 (1998), pp. 195–210.

[47] Annamarie E. Allen and Jason W. Locasale. "Glucose Metabolism in Cancer: The Saga of Pyruvate Kinase Continues". In: *Cancer Cell* 33.3 (2018), pp. 337–339.

[48] William J Israelsen and Matthew G Vander Heiden. "Pyruvate kinase: function, regulation and role in cancer". In: *Semin Cell Dev Biol* 43.1 (2015), pp. 43–51.

[49] Mohd Askandar Iqbal et al. "Pyruvate kinase M2 and cancer: An updated assessment". In: *FEBS Letters* 588.16 (2014), pp. 2685–2692.

[50] Barbara Chaneton et al. "Serine is a natural ligand and allosteric activator of pyruvate kinase M2". In: *Nature* 491.7424 (2012), pp. 458–462.

[51] Kirstie E Keller et al. "SAICAR induces protein kinase activity of PKM2 that is necessary for sustained proliferative signaling of cancer cells". In: *Molecular Cell* 53.5 (2014), pp. 700–709. eprint: `NIHMS150003`.

[52] Zongwei Li, Peng Yang, and Zhuoyu Li. "The multifaceted regulation and functions of PKM2 in tumor progression". In: *Biochimica et Biophysica Acta - Reviews on Cancer* 1846.2 (2014), pp. 285–296.

[53] Rob C Oslund et al. "Bisphosphoglycerate mutase controls serine pathway flux via 3- phosphoglycerate". In: *Nature Chemical Biology* 13.10 (2017), pp. 1081–1087.

[54] Ming Yan et al. "SAICAR activates PKM2 in its dimeric form". In: *Biochemistry* 55.33 (2016), pp. 4731–4736.

[55] Andrew D. James et al. "Cutting off the fuel supply to calcium pumps in pancreatic cancer cells: role of pyruvate kinase-M2 (PKM2)". In: *British Journal of Cancer* 122.2 (2020), pp. 266–278.

[56] Heather R Christofk et al. "The M2 splice isoform of pyruvate kinase is important for cancer metabolism and tumour growth". In: 452.March (2008).

[57] Yu huan Li et al. "PKM2, a potential target for regulating cancer". In: *Gene* 668.March (2018), pp. 48–53.

[58] E. B. Waygood and B. D. Sanwal. "The control of pyruvate kinases of Escherichia coli. I. Physicochemical and regulatory properties of the enzyme activated by fructose 1,6 diphosphate". In: *Journal of Biological Chemistry* 249.1 (1974), pp. 265–274.

[59] M. Markus et al. "Analysis of progress curves. Rate law of pyruvate kinase type 1 from Escherichia coli". In: *Biochemical Journal* 189.3 (1980), pp. 421–433.

[60] Joost Van Den Brink et al. "Dynamics of glycolytic regulation during adaptation of Saccharomyces cerevisiae to fermentative metabolism". In: *Applied and Environmental Microbiology* 74.18 (2008), pp. 5710–5723.

[61] Yi Fan Xu et al. "Regulation of Yeast Pyruvate Kinase by Ultrasensitive Allostery Independent of Phosphorylation". In: *Molecular Cell* 48.1 (2012), pp. 52–62.

[62] Bas Teusink and Douwe Molenaar. "Systems biology of lactic acid bacteria: For food and thought". In: *Current Opinion in Systems Biology* 6 (2017), pp. 7–13.

[63] M H N Hoefnagel et al. "Time dependent responses of glycolytic intermediates in a detailed glycolytic model of Lactococcus lactis during glucose run-out experiments". In: *Molecular Biology Reports* 29 (2002), pp. 157–161.

[64] Ettore Murabito et al. "Monte-Carlo Modeling of the Central Carbon Metabolism of Lactococcus lactis : Insights into Metabolic Regulation". In: 9.9 (2014).

[65] Johan H. Van Heerden. "Dynamic regulation of yeast glycolysis through trehalose cycling: a probabilistic view of metabolic transitions". In: (2016), pp. 1–132.

[66] Moez Bali and S. Randall Thomas. "A modelling study of feedforward activation in human erythrocyte glycolysis". In: *Comptes Rendus de l'Academie des Sciences - Serie III* 324.3 (2001), pp. 185–199.

[67] Kazuhiko Abbe and Tadashi Yamada. "Purification and Properties of Pyruvate Kinase from Streptococcus mutans". In: *Journal of Bacteriology* 149.1 (1982), pp. 299–305.

[68] Kazuhiko Abbe, Shoko Takahashi, and Tadashi Yamada. "Purification and Properties of Pyruvate Kinase from Streptococcus sanguis and Activator Specificity of Pyruvate Kinase from Oral Streptococci". In: 39.3 (1983), pp. 1007–1014.

[69] Nadine Veith et al. "Organism-Adapted Specificity of the Allosteric Regulation of Pyruvate Kinase in Lactic Acid Bacteria". In: *PLoS Computational Biology* 9.7 (2013).

[70] Bas Teusink et al. "Can yeast glycolysis be understood terms of vitro kinetics of the constituent enzymes? Testing biochemistry". In: *European Journal of Biochemistry* 267.17 (2000), pp. 5313–5329.

[71] Franco B. Du Preez et al. "From steady-state to synchronized yeast glycolytic oscillations I: Model construction". In: *FEBS Journal* 279.16 (2012), pp. 2823–2836.

[72] F.J Bruggeman, J.L Snoep, and B. Teusink. *Molecular Systems Biology.* 2012, p. 68.

[73] Marion M. Bradford. "A rapid and sensitive method for the quantitation of microgram quantities of protein utilizing the principle of protein-dye binding". In: *Analytical Biochemistry* (1976).

[74] Ilona Faustova and Jaak Järv. "Kinetic analysis of cooperativity of phosphorylated L-type pyruvate kinase". In: 1 (2006), pp. 179–189.

[75] Claudia N Morris, Stanley Ainsworth, and Julian Kinderlerer. "The regulatory properties of yeast pyruvate kinase". In: *Journal of Biochemistry* 217 (1984), pp. 641–647.

[76] Martin Peters et al. "The JWS online simulation database". In: *Bioinformatics (Oxford, England)* 33.10 (May 2017), pp. 1589–1590.

[77] Karl Josef Johannes and Benno Hess. "Allosteric kinetics of pyruvate kinase of Saccharomyces carlsbergensis". In: *Journal of Molecular Biology* 76.2 (1973), pp. 181–205.

[78] Manfred Rizzi et al. "In vivo analysis of metabolic dynamics in Saccharomyces cerevisiae: II. Mathematical model". In: *Biotechnology and Bioengineering* 55.4 (1997), pp. 592–608.

[79] A L Kiewiet et al. "Testing Biochemistry Revisited : How In Vivo Metabolism Can Be Understood from In Vitro Enzyme Kinetics". In: *PLoS Computational Biology* 8.4 (2012).

[80] Jacques Monod, Jeffries Wyman, and Jean-Pierre Changeux. "On the nature of Allosteric Transitions: A Plausible Model". In: *Journal of Molecular Biology* 12.December (1965), pp. 88–188.

[81] Archibald Vivian Hill. "The possible effects of the aggregation of the molecules of hæmoglobin on its dissociation curves". In: *The Journal of Physiology* 40 (Jan. 1910), pp. i–vii.

[82] Jan Hendrik S. Hofmeyr and Athel Cornish-Bowden. "The reversible hill equation: How to incorporate cooperative enzymes into metabolic models". In: *Bioinformatics* 13.4 (1997), pp. 377–385.

[83] Jorge L Galazzo and James E Bailey. "Fermentation pathway kinetics and immobilized Saccharomyces cerevisiae". In: *Enzyme and Microbial Technology* 12.March 10990 (1990), pp. 162–172.

[84] Petr Herman and J Ching Lee. "Functional Energetic Landscape in the Allosteric Regulation of Muscle Pyruvate Kinase I. Calorimetric Study". In: *Biochemistry* 48.40 (2009), pp. 9448–9455.

[85] Arno J. Hanekom et al. "Experimental evidence for allosteric modifier saturation as predicted by the bi-substrate Hill equation". In: *IEE Proceedings - Systems Biology* 153.November (2015), pp. 153–160.

[86] Johann M Rohwer, Arno J Hanekom, and Jan-hendrik S Hofmeyr. "A Universal Rate Equation for Systems Biology". In: *Molecular Cell* (2007), pp. 175–188.

[87] Arno J Hanekom. "Generic kinetic equations for modelling multisubstrate reactions in computational systems biology". In: *MSc Thesis, Stellenbosch University* January (2006).

[88] Inc. Wolfram Research. *Mathematica, Version 12.3.1*. Champaign, IL, 2021.

[89] Jacobus Barend Van Dyk. "Mathematical modelling of glycolysis in skeletal muscle cells". PhD thesis. 2020.

[90] Franco B. Du Preez, David D. Van Niekerk, and Jacky L. Snoep. "From steady-state to synchronized yeast glycolytic oscillations II: Model validation". In: *FEBS Journal* 279.16 (2013), pp. 2823–2836.